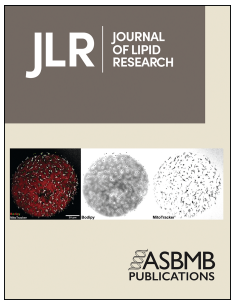

Role of Enterocyte *Enpp2* and Autotaxin in Regulating Lipopolysaccharide Levels, Systemic Inflammation and Atherosclerosis

Arnab Chattopadhyay, Pallavi Mukherjee, Dawoud Sulaiman, Huan Wang, Victor Girjalva, Nasrin Dorreh, Jonathan P. Jacobs, Samuel Delk, Wouter H. Moolenaar, Mohamad Navab, Srinivasa T. Reddy, Alan M. Fogelman

PII: S0022-2275(23)00043-3

DOI: https://doi.org/10.1016/j.jlr.2023.100370

Reference: JLR 100370

To appear in: *Journal of Lipid Research*

Received Date: 6 February 2023

Revised Date: 3 April 2023

Accepted Date: 7 April 2023

Please cite this article as: Chattopadhyay A, Mukherjee P, Sulaiman D, Wang H, Girjalva V, Dorreh N, Jacobs JP, Delk S, Moolenaar WH, Navab M, Reddy ST, Fogelman AM, Role of Enterocyte *Enpp2* and Autotaxin in Regulating Lipopolysaccharide Levels, Systemic Inflammation and Atherosclerosis, *Journal of Lipid Research* (2023), doi: https://doi.org/10.1016/j.jlr.2023.100370.

JLR-D-23-00066 R-1

Role of Enterocyte *Enpp2* and Autotaxin in Regulating Lipopolysaccharide Levels, Systemic Inflammation and Atherosclerosis

Arnab Chattopadhyay[1], Pallavi Mukherjee[1], Dawoud Sulaiman[1], Huan Wang[1], Victor Girjalva[1], Nasrin Dorreh[1], Jonathan P. Jacobs[2,4,5], Samuel Delk[1,6], Wouter H. Moolenaar[7], Mohamad Navab[1], Srinivasa T. Reddy[1,3,6*], and Alan M. Fogelman[1].

Department of Medicine, Division of Cardiology[1], The Vatche and Tamar Manoukian Division of Digestive Diseases[2], Department of Molecular and Medical Pharmacology[3], UCLA Microbiome Center[4], David Geffen School of Medicine at UCLA and the Division of Gastroenterology, Hepatology and Parenteral Nutrition, Veterans Administration Greater Los Angeles Healthcare System Los Angeles[5], Molecular Toxicology Interdepartmental Degree Program[6], Fielding School of Public Health, University of California, Los Angeles, CA 90095, USA; Division of Biochemistry, Netherlands Cancer Institute, Amsterdam, the Netherlands[7].

***Corresponding author**: Srinivasa T. Reddy, PhD, e-mail: sreddy@mednet.ucla.edu

Running Title: *Enterocyte Enpp2 and Autotaxin*

ABSTRACT

Conversion of lysophosphatidylcholine (LPC) to lysophosphatidic acid (LPA) by autotaxin, a secreted phospholipase D, is a major pathway for producing LPA. We previously reported that feeding *Ldlr*$^{-/-}$ mice standard mouse chow supplemented with unsaturated LPA or LPC qualitatively mimicked the dyslipidemia and atherosclerosis induced by feeding a Western diet (WD). Here we report that adding unsaturated LPA to standard mouse chow also increased the content of reactive oxygen species (ROS) and oxidized phospholipids (OxPL) in jejunum mucus. To determine the role of intestinal autotaxin, enterocyte specific *Ldlr*$^{-/-}$/*Enpp2* knockout (iKO) mice were generated. In control mice, the WD increased enterocyte *Enpp2* expression and raised autotaxin levels. *Ex vivo*, addition of OxPL to jejunum from *Ldlr*$^{-/-}$ mice on a chow diet induced expression of *Enpp2*. In control mice, the WD raised OxPL levels in jejunum mucus, and decreased gene expression in enterocytes for a number of peptides and proteins that affect antimicrobial activity. On the WD, the control mice developed elevated levels of LPS in jejunum mucus and plasma, with increased dyslipidemia and increased atherosclerosis. All of these changes were reduced in the iKO mice. We conclude that the WD increases the formation of intestinal OxPL, which i) induce enterocyte *Enpp2* and autotaxin resulting in higher enterocyte LPA levels; that ii) contribute to the formation of ROS that help to maintain the high OxPL levels; iii) decrease intestinal antimicrobial activity; and iv) raise plasma LPS levels that promote systemic inflammation and enhance atherosclerosis.

Key Words: Lysophospholipase D ● Lysophosphatidic acid (LPA) ● Atherosclerosis ● Oxidized phospholipids ● Small intestine ● Apolipoprotein A-I (apoA-I) mimetic peptides ● Transgenic tomatoes expressing the apoA-I mimetic peptide 6F (Tg6F).

INTRODUCTION

Lysophosphatidic acid (LPA) has emerged as an important signaling molecule in vascular disease (1, 2). LPA was found to mediate the rapid activation of platelets and endothelial cells induced by mildly oxidized LDL, and was present in human atherosclerotic lesions (3). Unsaturated LPA was found to release CXCL1 from endothelial cells, which was subsequently, immobilized on the cell surface to mediate LPA-induced monocyte adhesion, and systemic LPA accelerated the progression of atherosclerosis in mice (4). Blocking the LPA receptors 1 and 3 reduced hyperlipidemia-induced arterial leukocyte arrest and atherosclerosis in the presence of functional CXCL1, indicating that hyperlipidemia-induced monocyte recruitment depends on LPA (4). Mice deficient in LPA receptor 4 had about a 25% reduction in atherosclerotic lesion area in the proximal aorta and arch (5). Genome-wide association studies in humans identified single nucleotide polymorphisms in *PLPP3* (phospholipid phosphatase 3) as a novel locus associated with risk for coronary heart disease that was independent of traditional risk factors (6). The protein product of this gene is lipid phosphate phosphatase 3 (LPP3), which decreases the availability of bioactive lipids including LPA. Reductions in *Plpp3* expression in mice increased plasma LPA levels, increased atherosclerosis, and increased plaque associated LPA and inflammation (7).

LPA has also been shown to play a role in the clinical events that result from atherosclerosis. After acute myocardial infarction in both mice and humans, there was an increase in autotaxin activity, with increased levels of LPA and inflammatory cells in blood and cardiac tissue (8). Moreover, following acute myocardial infarction in an LPA gain of function model, *Plpp3* specific inducible knockout mice, LPA levels were further increased, and there was higher systemic and cardiac inflammation compared to littermate controls (8).

LPA not only plays an important direct role in cardiovascular disease (1-8), LPA also been shown to play an important role in gut homeostasis and inflammation. LPA regulates the proliferation and differentiation of intestinal epithelial cells (9). Lysophosphatidic acid receptor 1 is critical for intestinal epithelial homeostasis and wound closure (10). Additionally, LPA receptor 1 is important in maintaining

intestinal epithelial barrier function and susceptibility to colitis (11). Mice with global deletion of LPA receptor 1 had decreased expression of tight junction proteins in their intestine, reduced intestine barrier function and increased bacteria loads in the intestinal mucosa and peripheral organs (11). Moreover, these mice had increased susceptibility to develop colitis (11).

We previously reported that the levels of unsaturated LPA in the small intestine correlated with the extent of aortic atherosclerosis (12), and feeding a Western diet (WD) increased unsaturated LPA levels in the small intestine of *Ldlr*$^{-/-}$ mice (13). Adding unsaturated LPA to standard mouse chow to achieve levels of LPA in the small intestine comparable to levels seen on feeding a WD resulted in gene expression in the small intestine that was similar to that found on feeding a WD and was associated with dyslipidemia (13), systemic inflammation (13), and aortic atherosclerosis (14) that was qualitatively similar to that induced by feeding the mice a WD.

A major source of LPA is the conversion of lysophosphatidylcholine (LPC) to LPA by autotaxin (phospholipase D), which is the protein product of the *Enpp2* gene (15). Supplementing standard mouse chow with LPC 18:1 resulted in increases in unsaturated LPC 18:1 in jejunum equal to that seen on feeding *Ldlr*$^{-/-}$ mice a WD (16), increased jejunum LPA species (14), and also resulted in dyslipidemia similar to that seen on adding unsaturated LPA to chow. Moreover, adding a specific oral inhibitor (PF8380) of autotaxin to mouse chow together with LPC 18:1 reduced these changes suggesting that a significant portion of LPA was being derived from autotaxin-mediated hydrolysis of LPC 18:1 (14). Pancreatic phospholipase A_2 group 1B is secreted into the duodenum in response to fat in the diet and acts on dietary phospholipids to convert them to their LPC forms that are rapidly and efficiently taken up by the enterocytes of the small intestine (17).

Approximately two-thirds of the fatty acids in the WD used in our studies are saturated. After absorption, dietary phospholipids containing saturated fatty acids are remodeled in enterocytes via LPC acyltransferase 3 (*Lpcat3*). Feeding *Ldlr*$^{-/-}$ mice a WD or feeding them chow supplemented with unsaturated LPA equally induced gene expression for *Lpcat3* (14). The importance of phospholipid

remodeling and de novo synthesis of unsaturated LPC in small intestinal enterocytes in the induction of WD-mediated systemic inflammation was demonstrated in mice with intestinal specific knockout of stearoyl-Co-A desaturase-1 (*Scd1*) (18).

The interface between the lumen of the intestine, which is rich in bacteria, and the enterocytes is largely composed of mucus that is secreted by intestinal goblet cells. In the colon, there are two mucus layers; a very dense layer adjacent to the enterocytes that prevents the luminal bacteria from directly interacting with the enterocytes, and a loose layer on the luminal side of the dense layer. The bacteria in the colon reside in the loose layer (19,20). In the small intestine where fat absorption occurs, there is no dense inner layer and the loose mucus layer is much thinner; it is even intermittent in some areas. In the absence of the dense mucus layer in the small intestine, the separation of bacteria from enterocytes is dependent on antibacterial peptides and proteins that are secreted into the mucus to regulate the number of bacteria, and their interaction with the enterocytes (21).

We recently reported (22) that oxidized phospholipids in the small intestine cause changes in the mucus layer that result in increased lipopolysaccharide (LPS) levels in small intestine, and systemic inflammation (22). The 6F peptide is a member of a family of class A amphipathic helical peptides that bind oxidized phospholipids so avidly that they cannot interact with cells (23,24). When *Ldlr*$^{-/-}$ mice were fed a chow diet or a WD or a WD to which a concentrate of transgenic tomatoes expressing the 6F peptide (Tg6F) was added, the mucus levels of oxidized phospholipids in jejunum of mice receiving Tg6F did not increase beyond the levels seen on feeding the mice a chow diet (22).

After feeding the WD, gene expression in the jejunum decreased for multiple antimicrobial peptides and proteins that are secreted into the mucus layer of the jejunum (22). As expected with such changes, LPS levels in jejunum mucus increased, and there was an increase in LPS levels in the lymph draining the jejunum, and in the plasma of mice fed a WD compared to mice fed chow (22). Adding Tg6F to the WD reduced these WD-mediated changes (22).

Adding oxidized phospholipids *ex vivo* to the jejunum from mice fed a chow diet reproduced the changes in the expression of genes that control the intestinal levels of antimicrobial peptides and proteins *in vivo* in response to a WD (22), and adding the 6F peptide to the *ex vivo* incubations prevented the oxidized phospholipid-mediated changes (22).

The present study was designed to determine the role of LPA produced locally by autotaxin in enterocytes from *Ldlr*$^{-/-}$ mice in WD-induced dyslipidemia, systemic inflammation and atherosclerosis. The results demonstrate additional similarities to those previously reported (13,14) for feeding *Ldlr*$^{-/-}$ mice fed a WD compared to feeding them a chow diet supplemented with LPA. The present study also shows that enterocyte-specific deletion of the gene for autotaxin, *Enpp2*, produced results similar to those obtained on adding Tg6F to a WD that was fed to *Ldlr*$^{-/-}$ mice.

MATERIALS AND METHODS

Materials

Supplemental Table S1 shows the sources for ELISA assay kits. The apoA-I mimetic peptide 6F (12) and a control peptide (22) were described previously. Oxidized 1-palmitoyl-2-arachidonyl-*sn*-glycero-3-phosphocholine (Ox-PAPC) was purchased from Avanti Polar Lipids (catalog #870604P). Unless otherwise stated, other materials were from previously cited sources (22).

Mice and Diets

Enpp2$^{fl/fl}$ mice (25) were crossed with *Ldlr*$^{-/-}$ mice that were originally purchased from Jackson Laboratories on a C57BL/6J background and maintained in the breeding colony of the Department of Laboratory and Animal Medicine at the David Geffen School of Medicine at UCLA to generate *Enpp2*$^{fl/fl}$/ *Ldlr*$^{-/-}$ mice, which are referred to in this manuscript as "Cont." mice. The *Enpp2*$^{fl/fl}$/ *Ldlr*$^{-/-}$ mice were crossed with Villin Cre (*VilCre*) mice on a C57BL/6J background that were purchased from Jackson Laboratories (stock#004586) to ultimately yield *Enpp2*$^{fl/fl}$/ *Ldlr*$^{-/-}$*/VilCre* mice, which are referred to in this manuscript as "iKO" mice (intestinal knockout mice). *Enpp2*$^{fl/fl}$/ *Ldlr*$^{-/-}$ mice were bred with *Enpp2*$^{fl/fl}$/

Ldlr$^{-/-}$*/VilCre* mice and the progeny were genotyped to obtain the "Cont." and "iKO" mice that were used in the experiments. The mice had unlimited access to standard mouse chow (Ralston Purina Rodent Laboratory Chow catalog #5001; 4.5% fat by weight) prior to the start of experiments. As described previously (22), to ensure that the mice ate all of their food, during the experiments the mice did not have unlimited access to food. During the weeks when the mice were on the experimental diets, the mice were given precisely 4 grams of diet per mouse each night (each cage contained 4 mice; each cage received 16 grams of diet each night). When the mice were switched to a Western Diet (WD), it was from Envigo (catalog #TD88137; 21% fat by weight). After receiving the diets for two weeks or for 5 months, all four groups gained weight (Supplemental Figure S1). Mice receiving the WD had greater weight gain compared to chow, which at two weeks (Supplemental Figure S1A) was less in the iKO mice on the WD compared to control mice on the WD, but was not less after 5 months (Supplemental Figure S1B). This experimental design assured that all of the mice ate the same amount of food each day, and that all four groups (Cont. mice on chow; Cont. mice on WD; iKO mice on chow; iKO mice on WD) gained weight over the course of the experiment indicating that the caloric intake even on the chow diet was sufficient. The gender and number of mice in each group is stated in the figure legends or in a supplemental table. If the age range did not exceed 1 month (e.g. age 2 – 3 months), only the age range of the mice is stated. If the age range of the mice used in the experiment exceeded 1 month, the Mean ± SEM of the group's age in months is reported. In each experiment, the number of mice of each age was the same for each of the four groups. For example, if there were 16 mice per group with ages ranging between 4 and 7 months, there could be 4 mice age 4 months, 4 mice age 5 months, 4 mice age 6 months and 4 mice age 7 months in each of the four groups. In this example, the age of the mice would be stated as 5.5 ± 0.3 months. The UCLA Animal Research Committee approved all experiments prior to initiation of the study, and the UCLA Division of Laboratory Animal Medicine monitored the mice daily to ensure compliance with all applicable rules and regulations.

Tissue and Cell Collection

Collecting jejunum mucus and isolation of enterocytes from the same segment of jejunum- Jejunum mucus was collected as previously described (22). Enterocytes were prepared as described previously (22, 26), which yielded a purity of enterocytes of ~83% (26). For determination of autotaxin levels associated with enterocytes, highly purified enterocytes were prepared by flow cytometry. Twelve cm sections of the proximal jejunum from each mouse were flushed twice with ice-cold PBS, then inverted and the ends ligated with thread. Jejunum sections were then incubated with shaking at 37°C for 15 minutes in Buffer A (1.5 mM KCl, 96 mM NaCl, 8 mM KH_2PO_4, 27 mM sodium citrate, 5.6 mM Na_2HPO_4, pH 7.3, 0.1 mM PMSF, and 1 mM benzamidine), followed by 30 minutes shaking at 37°C in Buffer B (2.7 mM KCl, 137 mM NaCl, 1.5 mM EDTA, 1.5 mM KH_2PO_4, 8.1 mM Na_2HPO_4, pH 7.4, 0.5 mM DTT, 0.1 mM PMSF, and 1 mM benzamidine). The tissue was further vortexed gently in Buffer B to release the intestinal cells, followed by passing the cell suspension through a 70 µm cell strainer (Corning, catalog #352350). Approximately 15 million cells were then passed through EpCAM enriching microbeads (Miltenyi, catalog #130-105-958) and their corresponding LS columns (Miltenyi, catalog #130-042-401). EpCAM enrichment yielded approximately 5 million cells, which were then washed in FACS buffer (5% FBS in PBS). Cells were pelleted by centrifugation at 4°C and incubated for 45 minutes on ice with the following antibodies all of which were used at a 1:100 dilution: EpCAM (Biolegend, catalog #118206), CD45 (Biolegend, catalog #103108), CD44 (Biolegend, catalog #103006), CD31 (Invitrogen, catalog #46-0311-82), F4/80 (Invitrogen, catalog #48-4801-82), and LYVE1 (Invitrogen, catalog #48-0443-82). After the addition of antibodies, the cells were kept under foil to avoid photobleaching. Following antibody staining, the cells were washed twice, then re-suspended in FACS buffer before analysis on a FACSAria (BD). Compensation was performed with UltraComp eBeads (Invitrogen, catalog #01-3333-42). To sort enterocytes, gates were constructed relative to unstained control cells to sort for $EpCAM^+$ cells, while excluding the following populations: $CD45^+$, $CD44^+$, $CD31^+$, $F4/80^+$, $LYVE1^+$.

Ex Vivo Studies of Jejunum

After an overnight fast, the intestines of *Ldlr*$^{-/-}$ mice on a chow diet were gently washed with cold PBS being careful to avoid perforation. The jejunum was isolated and carefully cut into to 2 cm sections. The jejunum sections were cut open and added to tubes containing 1 mL of PBS or containing 1 mL of PBS with the additions described in the Figure Legends. The tubes were incubated at 37°C for 4 hours with gentle mixing on a nutating mixer. The tubes were centrifuged at 13,000 rpm at 4°C for 5 minutes. The supernatant was carefully aspirated, the tissue was homogenized for 15 seconds, and immediately frozen. The next day RNA was isolated for RT-qPCR as described below.

Assays

Determination of oxidized phospholipids in jejunum mucus- Oxidized phospholipids were determined in jejunum mucus using an ELISA with the E06 antibody (Avanti Polar Lipids, catalog #330001Sn), a PC-BSA standard (Biosearch Technologies, catalog #PC-1011-10), and a 1:10 dilution as described previously (22).

Isolation of RNA and Gene Expression Analysis- Total RNA was isolated from mouse enterocytes or from whole jejunum or from jejunum segments using a Qiagen RNA extraction kit (catalog #74106) according to the manufacturer's instructions. The yield and purity of the isolated RNA was determined using a Nano-Drop spectrophotometer. Samples for real time qPCR (RT-qPCR) had A260/A280 ratios between 1.9 and 2.05. First-strand cDNA was synthesized from 1 μg of total RNA using a cDNA synthesis kit (Bio-rad, catalog #1708890). The cDNA was diluted 1:10 with nuclease-free water. RT-qPCR was performed on a Bio-rad CFX96 real time PCR detection system using SYBR Green Supermix (Bio-Rad, catalog #1708880). Unless otherwise stated, relative abundance of mRNA was calculated by normalizing to glyceraldehyde 3-phosphate dehydrogenase (GAPDH). Primer sequences are shown in Supplemental Table S2.

Determination of proteins in jejunum mucus, in enterocytes, in whole jejunum and in plasma- Total protein concentrations were determined by the Bradford assay (Sigma Aldrich, catalog #B6-916) or by the Lowry method using a Pierce™ Modified Lowry Protein Assay Kit, (Thermofisher, catalog #23240) according to the manufacturer's instructions.

Unless otherwise stated, the levels of specific proteins were determined by ELISA using kits according to the instructions of the manufacturer as shown in Supplemental Table S1. For the determination of autotaxin protein, Western blots were performed and the intensity of the target proteins determined by scans. Briefly, highly purified enterocytes were prepared by flow cytometry as described above. Approximately, 1.5 million highly purified enterocytes from each condition were pelleted by centrifugation. Protein cell lysis buffer (15 μL) and an equal volume of 2X Laemmli sample buffer were added to the cell pellet. The samples were boiled for 5 minutes at 100°C and loaded on an SDS-PAGE gel 4-20% (Bio-Rad, catalog #4561094). Following electrophoresis, gels were transferred to a PVDF membrane with protein transfer buffer using a Semi dry transfer apparatus (Bio-rad). Autotaxin protein was determined by Western blot analysis. Primary antibody against autotaxin was from Santa Cruz Biotechnology, (catalog #sc-374222) and the secondary antibody was goat anti-mouse IgG that was obtained from MilliporeSigma (catalog #AP124P). The blots were stripped and re-probed with vinculin antibody (Sigma, catalog #V4139) and goat anti-mouse secondary antibody that was obtained from MilliporeSigma (catalog #AP124P). Protein was quantified by ImageJ analysis of the Western blot. Band intensity was measured in arbitrary units. To normalize for loading variation, the relative levels of autotaxin protein were calculated by dividing the autotaxin protein value by the corresponding value for vinculin protein.

Immunohistochemistry- Tissue sections were deparaffinized and antigen retrieval was performed with boiling in citrate buffer (10 mM in PBS, pH 6). Primary antibodies for mucin 2 (MUC2) (Santa Cruz Biotechnology, Catalog # sc15334), E-Cadherin (R&D systems, Catalog# AF748), and Lysozyme (Invitrogen, Catalog# PA5-16668) were added (1:200 dilution) to the sections in blocking buffer (10%

BSA) and incubated overnight at 4°C. The slides were washed twice with 1X PBS and then stained with secondary antibodies (Invitrogen, Catalog # A32814 and Catalog # A10042) and with DAPI (Invitrogen, Catalog #D1306) for 90 min at room temperature. The slides were washed 1X PBS followed by addition of mounting solution (ThermoFisher, Catalog # P36931) followed by a coverslip. The negative control omitted the primary antibodies. Images were captured on a Leica DMi8 microscope with either 10x or 20x objective and LAS X software used for acquisition. The number of Paneth cells per crypt was determined by counting 10 crypts on each of 4 different slides taken from 3 different mice per group so that 120 crypts were counted for each group. The same strategy was used for counting the goblet cells per crypt. To determine the goblet cells per villus, 10 villi were counted on each of 6 different slides taken from 3 different mice per group so that 180 villi were counted for each group. The average data for each of the 4 slides for each group (Paneth cells per crypt and goblet cells per crypt) or each of the 6 slides for each group (goblet cells per villus) from each of the 3 mice per group are shown in the figures.

Other Assays- Plasma was collected and lipids were determined as previously described (22). LPA was measured by mass spectrometry as described previously (14). LPS in jejunum mucus and plasma was determined using a LAL Chromogenic Endotoxin Quantitation Kit (Thermo Fisher Scientific Pierce, catalog #88282) following the manufacturer's instructions. Measurement of reactive oxygen species (ROS) in jejunum mucus, and plasma levels of IL-6 and serum amyloid A (SAA) were determined as described previously (22).

Statistical Analyses

In comparing more than two groups, ANOVA was performed and followed by multiple comparison tests using version 9.1.2 (GraphPad Software, San Diego, CA). In comparing two groups with an unpaired experimental design, the unpaired two-tailed *t* test was used and a correction (e.g. Welch's correction) was applied if the standard deviations were different. Statistical significance was considered achieved if $P < 0.05$. Unless otherwise stated, values are presented as the Mean ± SEM.

Almost all of the Figures and Supplemental Figures compare four different groups in each panel with each group shown as a bar graph. Reading figures from left to right in which Cont. mice on Chow or WD, and iKO mice on Chow or WD are compared, the first bar graph is Cont. mice on the chow diet (Chow-Cont.). The second bar graph is iKO mice on the chow diet (Chow-iKO). The third bar graph is Cont. mice on the WD (WD-Cont.). The fourth bar graph is iKO mice on the WD (WD-iKO). To facilitate the ability of the reader to see similarities and differences at a glance, Chow-Cont. is colored green. Chow-iKO is colored green unless it is significantly different from Chow-Cont. with the difference being in the same direction as the change in the WD-Cont. (e.g. if both Chow-iKO and WD-Cont. have values lower than Chow-Cont., both will have the same color as the WD-Cont.). WD-Cont. is rose colored unless it is not significantly different from Chow-Cont. in which case it is green. WD-iKO is rose colored unless it is not significantly different from Chow-Cont. or is different from the Chow-Cont. in the opposite direction to the change in the WD-Cont. in which case iKO will be colored green. The asterisks denote significant differences as indicated in the Figure Legends.

RESULTS

Adding unsaturated LPA to standard mouse chow increases ROS, oxidized phospholipids and LPS levels in jejunum mucus

We previously reported (13,14) that adding unsaturated LPA to normal mouse chow caused changes in *Ldlr*$^{-/-}$ mice that qualitatively mimicked feeding the mice a WD (e.g. dyslipidemia, systemic inflammation and aortic atherosclerosis). More recently, we reported that the WD mediates increases in the levels of ROS, oxidized phospholipids and LPS in jejunum mucus and plasma, which enhance WD-mediated dyslipidemia and systemic inflammation (22). Supplemental Figure S2 demonstrates that similar to feeding *Ldlr*$^{-/-}$ mice a WD, adding LPA 18:1 to standard mouse chow increased the levels of ROS, oxidized phospholipids and LPS in jejunum mucus and plasma.

***Enpp2* expression in enterocytes**

The protein product of *Enpp2*, autotaxin, plays a major role in the generation of LPA (25). As shown in **Figure 1** gene expression for enterocyte *Enpp2* was markedly decreased in the iKO mice compared to the Cont. mice after two weeks on the diets (**Figure 1A**) or after 5 months on the diets (**Figure 1B**). At both time points in the Cont. mice, *Enpp2* expression increased on the WD compared to the chow diet (Figure 1A and 1B). The residual *Enpp2* expression was likely due to non-enterocyte cells contaminating the preparations (26). Further purifying the enterocytes by flow cytometry followed by Western Blotting demonstrated the increase in autotaxin protein on the WD compared to the chow diet in the Cont. mice (**Figure 1C**). In contrast to jejunum enterocytes, hepatic expression of *Enpp2* was not altered in iKO mice confirming the specificity of the knockout (Supplemental Figure S3).

We recently reported that adding oxidized phospholipids *ex vivo* to jejunum from *Ldlr*$^{-/-}$ mice fed a chow diet reproduced the changes in expression of genes that determine intestinal levels of antimicrobial peptides and proteins (22). In those studies, we demonstrated that adding the apoA-I mimetic peptide (6F) prevented these changes in gene expression (22). However, we did not study the expression of *Enpp2* in our previous studies (22). As shown in Supplemental Figure S4, adding oxidized phospholipids *ex vivo* to jejunum from *Ldlr*$^{-/-}$ mice fed a chow diet increased gene expression for *Enpp2* similar to what was seen *in vivo* in Cont. mice fed the WD (Figure 1). Moreover, adding the 6F peptide (but not a control peptide) prevented the increase in gene expression for *Enpp2* that was induced by the oxidized phospholipids (Supplemental Figure S4).

LPA levels in jejunum enterocytes

On the chow diet, enterocyte levels for LPA 16:0 (**Figure 2A**), LPA 18:0 (**Figure 2B**), LPA 18:1(**Figure 2C**) or LPA 18:2 (**Figure 2D**) were not different in Cont. compared to iKO mice. On the WD in the Cont. mice, there was an increase in enterocyte levels for LPA 16:0, LPA 18:1 and LPA 18:2 compared to the chow diet; the levels for LPA 18:0 were not different by diet or genotype. In the iKO

mice on the WD, the levels of LPA 16:0 and LPA 18:2 did not increase above those seen in mice on the chow diet. Enterocyte levels of LPA 18:1 increased on the WD in both Cont. and iKO mice, but the levels in the iKO mice were substantially less than in the Cont. mice on the WD.

Oxidized phospholipid levels in jejunum mucus

The data from the Cont. mice shown in **Figure 3** confirm our previous report (22) regarding the increase in oxidized phospholipids in jejunum mucus from *Ldlr*$^{-/-}$ mice fed a WD. Figure 3 also demonstrates that on the chow diet there was no difference in the level of oxidized phospholipids in jejunum mucus from Cont. or iKO mice. However, while the Cont. mice showed an increase in the levels of oxidized phospholipids in jejunum mucus on the WD, the levels of oxidized phospholipids in the mucus of the iKO mice on the WD were not significantly different from those seen in the chow-fed mice (Figure 3). These data together with the data in Figure 2 and Supplemental Figure S2 and Figure 1C are correlative suggesting that the increased levels of oxidized phospholipids in jejunum mucus in *Ldlr*$^{-/-}$ mice fed a WD may be due, at least in part, to the local generation of LPA by enterocyte autotaxin.

Gene expression in jejunum enterocytes for peptides and proteins that affect antimicrobial activity

We previously reported (22) that when *Ldlr*$^{-/-}$ mice were fed a WD, the expression of 22 genes that directly or indirectly regulate the levels of intestinal antimicrobial peptides and proteins decreased, and the expression of two genes increased. Adding Tg6F to the WD reduced these changes (22). The protein products of many of these genes are produced in goblet and/or Paneth cells. Two important factors required for the formation of goblet and Paneth cells are the basic helix-loop-helix transcription factor atonal homolog 1 (*Atoh1*) that is also known as *Math1* (27-29), and growth factor independent protein 1 (*Gfi1*), a zinc-finger protein family member that is a direct target gene of *Atoh1*, and is required for the formation of Paneth cells (30). Notch pathway genes are also important for the production of intestinal antimicrobial peptides and proteins (31-33). **Figure 4A** and Supplemental Table S3 present data for 17 of the 22 genes that previously showed decreased gene expression on the WD in *Ldlr*$^{-/-}$ mice with wild-type

Enpp2 (22). **Figure 4B** and supplemental Table S3 present data for two genes that previously showed increased gene expression on the WD in *Ldlr*$^{-/-}$ mice with wild-type *Enpp2* (22); lipopolysaccharide-binding protein (*Lbp*) and *Spp1* whose gene product is osteopontin. The data in Figures 4A and 4B are presented as a heat map. Figure 4A confirms a decrease in gene expression in the jejunum of the Cont. mice fed a WD for 15 of the 17 genes that were previously seen to decrease on the WD (22). In the present studies, in contrast to the previous studies (22), gene expression for surfactant A (*Sftpa1*) and defensin 3 (*Defb3*) did not significantly change on the WD (Figure 4A and Supplemental Table S3). The data from the Cont. mice in Figure 4B confirm our previous observation (22) that gene expression for *Lbp* and *Spp1* increased on the WD and demonstrate results similar to those reported (22) after adding Tg6F to the WD, i.e. enterocyte-specific KO of *Ennp2* prevented the increased expression of these two genes on the WD. Seventeen of the 19 genes in Figures 4A and 4B showed a significant difference between iKO mice that were fed the chow diet and Cont. mice that were fed the WD (Supplemental Table S3). Ten of the 19 genes showed a significant difference between Cont. mice that were fed the WD and iKO mice that were fed the WD, and in one additional gene (*Defb4*) significance was almost achieved ($P = 0.0560$). In six genes in which the difference between Cont. mice that were fed the WD and iKO mice that were fed the WD did not reach statistical significance, gene expression in the Cont. mice fed the WD was significantly decreased compared to Cont. mice fed the chow diet (supplemental Table S3).

Determination of peptide and protein levels that affect antimicrobial activity, and quantification of the cells that produce these peptides and proteins

On the WD, protein levels for ATOH1 that is required for the formation of goblet and Paneth cells were significantly increased in the iKO mice (**Figure 5A**). On the WD in Cont. mice, protein levels of GFI1, which is required for the formation of Paneth cells were decreased, but there was no decrease in GFI1 in the iKO mice (**Figure 5B**). By immunohistochemistry, the number of goblet cells/villus were increased in iKO mice on the WD compared to Cont. mice on the chow diet (**Figure 5C**), and goblet cells/crypt showed a trend to less of a decrease in iKO mice on the WD compared to Cont. mice on the

WD (**Figure 5D**). Paneth Cells in the iKO mice were increased compared to the Cont. mice on both the chow diet and the WD (**Figure 5E**).

Figure 6 shows that on the WD in the Cont. mice compared to iKO mice, protein levels in the jejunum were decreased for IL-36γ (Figure 6A), IL-23 (Figure 6B) and IL-22 (Figure 6C), which are critical for antimicrobial activity in the intestine (22). In each instance, these changes were prevented or the decrease was less in the iKO mice on the WD. On the chow diet, both IL-23 and IL-22 were decreased in the iKO mice (Figures 6B and 6C), which suggests that the control of IL-23 and IL-22 levels may be more complex than that for IL-36γ. On the WD, lysozyme protein levels in jejunum mucus were decreased in both Cont. and iKO mice (Figure 6D) indicating that *Enpp2* knockout in enterocytes did not improve the WD-mediated decrease in lysozyme protein levels. On the WD in the Cont. mice (but not in the iKO mice) protein levels in jejunum mucus were decreased for the major intestinal mucus protein, MUC2 (Figure 6E).

Figure 7 demonstrates that on the WD in the Cont. mice, protein levels in the jejunum were decreased for NOTCH2 (Figure 7A) and the Notch ligand DLL4 (Figure 7B); these WD-mediated changes were prevented in the iKO mice. On the WD in both the Cont. and iKO mice, APOA-I proteins levels were decreased in jejunum mucus (Figure 7C). On the WD in the Cont. mice, jejunum mucus levels for LBP increased, but the increase was much less in the iKO mice (Figure 7D).

LPS levels increased in jejunum mucus on the WD, but increased much less in iKO mice.

LPS levels increased in jejunum mucus on the WD compared to the chow diet. On the WD, LPS levels in iKO mucus increased much less than in Cont. mucus (**Figure 8**). Supplemental Figure S5 demonstrates that the LPS content of the chow diet was substantially higher than that of the WD indicating that the increased levels of LPS in jejunum mucus on the WD were not due to LPS in the diet.

Plasma total cholesterol, triglycerides and apoA-I levels after two weeks on chow or WD

As shown in **Figure 9** after two weeks on the chow diet there was no difference between the levels of plasma total cholesterol (Figure 9A) or plasma triglycerides (Figure 9B) in Cont. compared to iKO mice. However, plasma apoA-I levels were higher in iKO mice compared to Cont. mice on the chow diet (Figure 9C). Plasma total cholesterol levels increased in both Cont. and iKO mice on the WD, but increased less in the iKO mice (Figure 9A). Plasma triglyceride levels increased in the Cont. mice on the WD, but did not increase in iKO mice (Figure 9B). Plasma apoA-I levels decreased on the WD in both Cont. and iKO mice, but decreased less in the iKO mice compared to the Cont. mice (Figure 9C). On the chow diet, HDL-cholesterol levels were higher in iKO mice. On the WD, HDL-cholesterol levels were decreased in both Cont. and iKO mice, but decreased less in the iKO mice (Supplemental Figure S6).

Plasma LPA levels after two weeks on chow or WD

Figure 10 demonstrates that in contrast to jejunum LPA levels, there was no genotype effect in plasma after two weeks on the chow or WD. Moreover, after two weeks on the diets, there was no change in the levels of plasma LPA 16:0 (Figure 10A) or LPA 18:0 (Figure 10B) on the WD compared to the chow diet. Both Cont. and iKO mice had increased levels of LPA 18:1 in plasma on the WD compared to the chow diet, but in contrast to the case in jejunum where the iKO mice had less of an increase on the WD (Figure 2C), there was no difference in plasma LPA 18:1 levels (Figure 10C). Plasma levels of LPA 18:2 on the WD decreased compared to chow, and there was no difference between Cont. and iKO mice (Figure 10D), which was distinctly different from the case in the jejunum where LPA 18:2 increased on the WD in Cont. mice compared to the chow diet, but remained the same as in chow-fed mice in the iKO mice on the WD (Figure 2D).

Plasma LBP, LPS, IL-6 and SAA after two weeks on chow or WD

As shown in **Figure 11**, plasma levels of LBP and LPS increased on the WD compared to the chow diet, and on both chow and the WD there were lower plasma levels of LBP and LPS in iKO mice compared to Cont. mice (Figures 11A and 11B, respectively). Paralleling these changes, plasma levels of

IL-6 and SAA were higher in mice on the WD compared to the chow diet, and the levels were lower in iKO mice on the WD compared to Cont. mice (Figures 11C and 11D, respectively).

Changes after 5 months on chow or WD

The levels of plasma total cholesterol, triglycerides and apoA-I after feeding the diets for five months are shown in Supplemental Figure S7. The changes in plasma cholesterol, triglycerides and apoA-I after five months on the diets were similar to the changes after two weeks, except that the plasma cholesterol levels in the iKO mice on the WD (345 ± 24 mg/dL) compared to Cont. mice on chow (267 ± 14) did not quite reach statistical significance (P =0.0712).

Plasma LPA levels are shown in Supplemental Figure S8. Plasma LPA 16:0 and LPA 18:0 levels after feeding the diets for five months were lower in the mice receiving WD compared to mice receiving chow, but were not different between Cont. and iKO mice. After five months, plasma levels of LPA 18:1 remained higher on WD compared to chow, but in contrast to the case at two weeks, they were lower in the iKO mice on WD compared to Cont. mice on WD. After five months, LPA 18:2 levels remained lower on the WD compared to chow, and they were significantly lower in the iKO mice on WD compared to Cont. mice on WD.

Plasma levels of LBP, LPS, and SAA are shown in **Figure 12**. On the chow diet, plasma levels of LBP were lower in the iKO mice compared to the Cont. mice (Figure 12A). Plasma levels of LBP increased after five months on the WD compared to the chow diet in Cont. mice, but were not different from chow in iKO mice on the WD (Figure 12A). Plasma LPS levels increased after five months on the WD in Cont. mice, but in iKO mice on the WD, plasma LPS levels were not different from Cont. mice on the chow diet (Figure 12B). SAA levels increased after five months on the WD and increased less in the iKO mice (Figure 12C).

After five months on the WD, there was less of an increase in the iKO mice for the following parameters: percent of whole aorta with atherosclerotic lesions (**Figure 13A**); aortic root Oil Red O lesion

area (**Figure 13B**); area positive for macrophages (CD68) (**Figure 13C)**. As shown in Supplemental Figure S9 plasma levels of LPS significantly correlated with the data in Figure 13.

DISCUSSION

The epithelium of the intestine turns over every ~3-5 days. Thus, the proliferation and differentiation of intestinal epithelial cells is critical for maintenance of the epithelial barrier in the intestine. Konno et al. (9) demonstrated that LPA 18:1 plays an important role in the proliferation and differentiation of intestinal epithelial cells. Unsaturated LPA species including LPA 18:1 are the preferred ligands for LPA receptors 1, 2,3,4, 5, GPR87, P2Y5, P2Y10, and GPR35 (59). Yun and colleagues (10,11) demonstrated that LPA receptor 1 is important for intestinal epithelial homeostasis, wound closure, intestinal epithelial barrier function including preventing the entry of gut-bacteria, and susceptibility to colitis. The LPA species that Yun and colleagues (11) used in their experiments was also LPA 18:1. Orally administering LPA 18:1 as in the current study or LPA 18:2 (13, 14) at a dose of 1 μg per mg chow resulted in LPA levels in the small intestine of mice that were similar to those achieved by feeding a WD, and mimicked many of the changes induced by the WD including causing aortic atherosclerosis that was qualitatively the same as that seen on the WD (14). The levels of unsaturated phospholipids in enterocytes on the WD are largely not derived from unsaturated phospholipids in the WD. Indeed, we found that the chow diet contained dramatically more unsaturated phospholipids compared to the WD, especially 18:1 containing phospholipids (16). The WD mainly contains saturated fatty acids; it induces the expression of *Scd1* (18) and *Lpcat3* in enterocytes (14), which provide the unsaturated phospholipid substrates that are acted upon by enterocyte autotaxin, and likely accounts for most of the increased unsaturated LPA in enterocytes from mice on the WD.

Similar to our reports, Zhou et al. (4) reported that unsaturated LPA but not saturated LPA (18:0) accelerated the progression of atherosclerosis in mice. In our previous studies adding Tg6F to the WD reduced the levels of these LPA species in the jejunum and reduced the WD-induced changes (13,14). In the current studies, the response to the WD by the iKO mice was remarkably similar to that previously

reported in *Ldlr*$^{-/-}$ mice that were wild-type for *Enpp2* that were fed a WD that was supplemented with Tg6F (22). When administered orally, the 6F peptide is not absorbed intact, but is found intact in the lumen of the small intestine (12). Therefore, after oral administration, it must act in the vicinity of the enterocytes. The apoA-I mimetic peptide 6F is known to bind oxidized phospholipids such that they can no longer interact with cells (23). Supplemental Figure S4 shows that adding oxidized phospholipids to jejunum *ex vivo* induced *Enpp2* expression, which was prevented by adding the 6F peptide. The 6F peptide is one of three class A 18-amino acid residue apoA-I mimetic peptides (4F, 5F and 6F) that bind a number of lipids with much higher affinity than native apoA-I (23, 24). Unsaturated LPA is among the lipids bound by this class of apoA-I mimetic peptides with extraordinarily high affinity (60). Therefore, it is possible that oral 6F acts in part by binding and reducing the levels of both LPA and oxidized phospholipids in enterocytes.

The results in Figure 1 demonstrating that the WD induced the expression of *Enpp2* in enterocytes in Cont. mice are similar to the findings of Dusaulcy et al. (61) showing that expression of *Enpp2* in subcutaneous, perigonadal and perirenal adipose tissue was significantly increased in *Enpp2* wild-type mice fed a high-fat diet compared to when these mice were fed standard mouse chow. However, Dusaulcy et al. (61) did not see an increase in expression of *Enpp2* in brown adipose tissue, or brain or kidney on the high-fat diet, demonstrating that local factors and specific tissue characteristics determine *Enpp2* expression. Dusaulcy et al. (61) did not measure the levels of oxidized phospholipids in their studies. They did see a 38% decrease in total plasma LPA levels on knockout of adipose-tissue specific *Enpp2* in chow-fed control mice, and there was a 62% increase in total plasma LPA levels on the high-fat diet compared to the chow diet in control mice, but not in the adipose-specific knockout mice. They did not measure individual LPA species. In our studies, after two weeks only LPA 18:1 levels increased in plasma on the WD compared to the chow diet, and there was no difference between the response of Cont. and iKO mice. However, after two weeks of feeding the diets, the plasma data were quite different from the enterocyte data. After two weeks, Cont. enterocyte levels of LPA 16:0, LPA 18:1

and LPA 18:2 were increased on the WD and were significantly less in the iKO enterocytes indicating that the changes in the intestine at this time point were not reflected in the plasma. In contrast to the results after two weeks of feeding the diets, after feeding the diets for five months, the iKO mice on the WD had significantly lower levels of plasma LPA 18:1 and LPA 18:2 compared to Cont. mice on WD. Dusaulcy et al. (61) measured plasma LPA levels after 13 weeks on the diets. Thus, periods longer than two weeks may be required for tissue-specific knockouts of autotaxin to be reflected in plasma LPA levels. Future studies measuring plasma autotaxin levels together with plasma LPA levels as a function of the time that the diets are fed will be required to determine if this is the case.

Brandon et al. (62) generated a different adipose-specific knockout of *Enpp2* than the one used by Dusaulcy et al. (61). Kraemer et al. (63) used the adipose-specific knockout of *Enpp2* that was generated by Brandon et al. (62) and found that it prevented the increase in LPA associated with LDL in genetically hyperlipidemic mouse models. We did not measure LPA levels in LDL.

We previously reported that adding unsaturated LPC to standard mouse chow qualitatively mimicked many of the features of feeding a WD to *Ldlr*$^{-/-}$ mice (14) and was similar to adding unsaturated LPA to standard mouse chow (13). In those studies (14), adding an inhibitor of autotaxin (PF8380) partially prevented the ability of unsaturated LPC added to mouse chow to mimic the WD. Since PF8380 is absorbed and acts in many tissues, the role of the intestine could not be determined (14). The current studies unequivocally demonstrate that LPA generated locally in the intestine plays an important role in the WD-mediated uptake of gut-derived LPS, systemic inflammation and enhanced atherosclerosis in *Ldlr*$^{-/-}$ mice.

Lin et al. (64) used inducible whole-body deletion of *Enpp2* in adult mice to study colitis. They reported that whole-body deletion of *Enpp2* suppressed experimental colitis, and that B cells were a major source of autotaxin in the colon. Kim et al. (65) reported that macrophages from myeloid cell lineage-restricted *Enpp2* knockout mice had reduced TLR4 complex formation that was associated with attenuation of phagocytosis, and iNOS expression. These mice exhibited increased bacterial content in

intestinal mucosa, and when bred with global *Il10*$^{-/-}$ mice on a C57BL/6 background for at least 8 generations, they exhibited accelerated colitis. The authors concluded that myeloid cell lineage autotaxin deficiency compromises innate immune responses, thereby promoting microbe-associated gut inflammation (65). These authors did not use this model to study atherosclerosis.

Karshovska et al. (66) reported that a tamoxifen-induced endothelial cell-specific *Enpp2* knockout decreased the following: atherosclerosis plaque area, macrophages in lesions, monocyte adhesion, and endothelial expression of C-X-C motif chemokine ligand 1 (CXCL1) in male and female *Apoe*$^{-/-}$ mice. *In vitro*, they found that *Enpp2* mediated mildly oxidized LDL-induced expression of CXCL1 in aortic endothelial cells by generating LPA 20:4, LPA 16:0 and LPA 18:1. Autotaxin was detected on the endothelial surface by confocal imaging. The expression of endothelial *Enpp2* was strongly correlated with plasma levels of LPA16:0, LPA 18:0 and LPA18:1 and aortic plaque size. These authors concluded that endothelial autotaxin promotes atherosclerosis and endothelial inflammation in a sex-independent manner that might be due to the generation of LPA20:4, LPA16:0 and LPA18:1 from mildly oxidized lipoproteins located on the endothelial surface (66). We previously demonstrated that the biologic activity of mildly oxidized LDL was largely due to its content of oxidized phospholipids (67-70). Karshovska et al. (66) did not report on oxidized phospholipids in their study.

The limitations of the data reported here included the following. In every experiment, mice of the same gender were compared (i.e. males and females were not mixed in any experiment), and each group being compared was closely matched for age. The data from these studies demonstrate that both male and female mice showed changes consistent with a role of enterocyte *Enpp2* in the parameters measured. However, because we used either male or female mice in each experiment (but not both in the same experiment), our data do not provide a quantitative comparison of male and female mice for all of the parameters measured, and therefore, we cannot exclude that there may be quantitative gender-based differences for some of the parameters measured. Similarly, although the ages of the mice used in these studies were carefully matched in every experiment, we did not measure every parameter by age in both

males and females, and therefore, we cannot exclude the possibility that there may be age-based differences for some of the parameters, nor can we provide a definitive picture of how each parameter changes with age.

Smyth et al. (71) made the case for autotaxin-derived LPA playing a role in the development and complications of atherosclerosis. The studies presented here provide support for this hypothesis, and show that targeting enterocyte *Enpp2* reduced WD-mediated increases in plasma LPS, dyslipidemia and aortic atherosclerosis in *Ldlr*$^{-/-}$ mice. **Figure 14** presents a schematic diagram that combines our previous data (12-14, 16, 18, 22) with the data presented here to show potential mechanisms for the role of enterocyte *Enpp2* in these processes.

GRANT SUPPORT

This work was supported in part by US Public Health Service Research Grant 1R01 HL148286 (A.M.F.) and the Laubisch, Castera, and M.K. Grey Funds at the University of California at Los Angeles. J.P.J. was supported by VA CDA2 IK2CX001717 and NIH/NIDDK P30 DK041301.

CONFLICT OF INTEREST

A.M.F, M.N., and S.T.R. were principals in Bruin Pharma and A.M.F. was an officer in Bruin Pharma during the course of some of these studies.

DATA AVAILABILITY

The data described in this manuscript are all contained within the manuscript. The reagents and transgenic animals can be shared upon request, by contacting either STR at sreddy@mednet.ucla.edu or AMF at amfogelman@mednet.ucla.edu

REFERENCES

1. Abdel-Latif, A., Heron, P.M., Morris, A.J., and Smyth, S.S. (2015) Lysophospholipids in coronary artery and chronic ischemic heart disease. *Curr Opin Lipidol* 26:432-437.

2. Smyth, S.S., Kraemer, M., Yang. L., Van Hoose, P., and Morris, A.J. (2020) Roles for lysophosphatidic acid signaling in vascular development and disease. *BBA – Molecular and Cell Biology of Lipids*. 1865:158734.

3. Siess, W., Zangl, K.J., Essler, M., Bauer, M., Brandl, R., Corrinth, C., Bittman, R., Tigyi, G., and Aepfelbacher, M. (1999) Lysophosphatidic acid mediates the rapid activation of platelets and endothelial cells by mildly oxidized low density lipoprotein and accumulates in human atherosclerotic lesions. *Proc Natl Acad Sci USA* 96:6931-6936.

4. Zhou, Z., Subramanian P., Sevilmis, G., Globke, B., Soehnlein, O., Karshovska, E., Megens, R., Heyll, K., Chun, J., Saulnier-Blache, J.S., Reinholz, M., van Zandvoort, M., Weber, C., Schober, A. (2011) Lipoprotein-derived lysophosphatidic acid promotes atherosclerosis by releasing CXCL1 from the endothelium. *Cell Metab*. 13:592-600.

5. Yang, L., Kraemer, M., Fang, X.F., Angel, P.M., Drake, R.R., Morris, A.J., and Smyth, S.S. (2019) LPA receptor 4 deficiency attenuates experimental atherosclerosis. *J Lipid Res*. 60: 972-980.

6. Schunkert, H., Konig, I.R., Kathiresan, S., Reilly, M.P., Assimes, T.L., Holm, H., Preuss, M., Stewart, A.F., Barbalic, M., Geiger, C., et al; Cardiogenics; CARDIo-GRAM Consortium. (2011) Large-scale association analysis identifies 13 new susceptibility loci for coronary artery disease. *Nat Genet*. 43:333-338.

7. Mueller, P.A., Yang, L., Ubele, M., Mao, G., Brandon, J., Vandra, J., Nichols, T.C., Escalante-Alcalde, D., Morris, A.J., and Smyth, S.S. (2019) Coronary artery disease risk-associated Plpp3 gene and its product lipid phosphate phosphatase 3 regulate experimental atherosclerosis. *Arterioscler Thromb Vasc Biol*. 39:2261-2272.

8. Tripathi, H., Al-Darraji, A., Abo-Aly, M., Peng, H., Shokri, E., Chelvarajan, Donahue, R.R., Levitan, B.M., Gao, E., Hernandez, G., Morris, A.J., Smyth, S.S., and Abdel-Latif, A. (2020) Autotaxin inhibition reduces cardiac inflammation and mitigates adverse cardiac remodeling after myocardial infarction. *J Mol Cell Cardiol*. 149:95-114.

9. Konno, T., Kotani, T., Setiawan, J., Nishigaito, Y., Sawada, N., Imada, S., Saito, Y., Murata, Y., and Matozaki, T. (2019) Role of lysophosphatidic acid in proliferation and differentiation of intestinal epithelial cells. *PLoS ONE*. 14:e0215255.
10. Lee, S-J., Leoni, G., Neumann, P-A., Chun, J., Nusrat, A., and Yun C.C. (2013) Distinct phospholipase C-β isozymes mediate lysophosphatidic receptor 1 effects on intestinal epithelial homeostasis and would closure. *Mol Cell Biol*. 33:2016-2028.
11. Lin, S., Han, Y., Jenkin, K., Lee, S-J., Sasaki, M., Klapproth, J-M., He, P., and Yun, C.C. (2018) Lysophosphatidic acid receptor 1 is important for intestinal epithelial barrier function and susceptibility to colitis. *Am J Pathol*. 188: 353-366.
12. Chattopadhyay, A., Navab, M., Hough, G., Gao, F., Meriwether, D., Grijalva, V., Springstead, J.R., Palgunachari, M.N., Namiri-Kalantari, R., Su, F., Van Lenten, B. J., Wagner, A.C., Anantharamaiah, G.M., Fairas-Eisner, R., Reddy, S.T., Fogelman, A.M. (2013) A novel approach to oral apoA-I mimetic therapy. *J Lipid Res*. **54**: 995-1010.
13. Navab, M., Hough, G., Buga, G.M., Su, F., Wagner, A.C., Meriwether, D., Chattopadhyay, A., Gao, F., Farias-Eisner, R., Smyth, S.S., Reddy, S.T., Fogelman, A.M. (2013) Transgenic 6F tomatoes act on the small intestine to prevent systemic inflammation and dyslipidemia caused by Western Diet and intestinally derived lysophosphatidic acid *J Lipid Res*. **54**: 3403-3418.
14. Navab, M., Chattopadhyay, A., Hough, G., Meriwether, D., Fogelman, S.I., Wagner, A.C., Grijalva, V., Su, F., Anantharamaiah, G.M., Hwang, L.H., Faull, K.F., Reddy, S.T., Fogelman, A.M. (2015) Source and role of intestinally derived lysophosphatidic acid in dyslipidemia and atherosclerosis. *J Lipid Res*. **56**: 871-887.
15. Aoki, J., Inoue, A., and Okudaira, S. (2008) Two pathways for lysophosphatidic acid production. *Biochim Biophys Acta* 1781:513-518.
16. Chattopadhyay, A., Navab, M., Hough, G., Grijalva, V., Mukherjee, P., Fogelman, H.R., Hwang, L.H., Faull, K.F., Lusis, A.J., Reddy, S.T., Fogelman, A.M. (2016) Tg6F ameliorates the increase

in oxidized phospholipids in the jejunum of mice fed unsaturated LysoPC or WD. *J Lipid Res*. **57**: 832-847.

17. Hui, D.Y. (2012) Phospholipase A2 enzymes in metabolic and cardiovascular diseases. *Curr Opin Lipidol*. 23:235-240.
18. Mukherjee, P., Hough, G., Chattopadhyay, A., Grijalva, V., O'Connor, E.I., Meriwether, D., Wagner, A., Ntambi, J.M., Navab, M., Reddy, S.T., Fogelman, A.M. (2018) Role of enterocyte stearoyl-Co-A desaturase-1 in LDLR-null mice. *J Lipid Res*. **59**: 1818-1840.
19. Johansson, M.E.V., Phillipson, M., Petersson, J., Velich, A., Holm, L., Hansson, G.C. (2008) The inner of the two Muc2 mucin-dependent mucus layers in colon is devoid of bacteria. *PNAS* **105**:15064-15069.
20. Johansson, M.E.V., Holmen Larsson, J.M., Hansson G.C. (2011) The two mucus layers of colon are organized by the MUC2 mucin, whereas the outer layer is a legislator of host-microbial interactions. *PNAS* **108**:4659-4665.
21. Ermund, A., Schutte, A., Johansson, M.E.V., Gustafsson, J.K., Hansson, G.C. (2013) Studies of mucus in mouse stomach, small intestine and colon. I. Gastrointestinal mucus layers have different properties depending on location as well as over Peyer's patches. *Am J Physiol Gastrointest Liver Physiol*. 305: G341-G347.
22. Mukherjee, P., Chattopadhyay, A., Grijalva, V., Dorreh, N., Lagishetty, V., Jacobs, J.P., Clifford, B.L., Vallim, T., Mack, J.J., Navab, M., Reddy, S.T., Fogelman, A.M. (2022) Oxidized phospholipids cause changes in jejunum mucus that induce dysbiosis and systemic inflammation. *J Lipid Res*. 63:100153.
23. Datta, G., Chaddha, M., Hama, S., Navab, M., Fogelman, A.M., Garber, D.W., Mishra, V.K., Epand, R.M., Epand, R.F., Lund-Katz, S., Phillips, M.C., Segrest, J.P., and Anantharamaiah, G.M. (2001) Effects of increasing hydrophobicity on the physical-chemical and biological properties of a class A amphipathic helical peptide. *J Lipid Res*. **42**:1096-1104.

24. Van Lenten, B.J., Wagner, A.C., Jung, C-L., Ruchala, P., Waring, A.J., Lehrer, R.I., Watson, A.D., Hama, S., Navab, M., Anantharamaiah, G.M., and Fogelman, A.M. (2008) Anti-inflammatory apoA-I mimetic peptides bind oxidized lipids with much greater affinity than human apoA-I. *J Lipid Res*. **49**:2302-2311.

25. Van Meeteren, L.A., Ruurs, P., Stortlers, C., Bouwman, P., van Rooijen, M.A, Pradere, J.P., Pettit, T.R., Wakelam, M.J.O., Saulnier-Blache, J.S., Mummery, C.L., Moolenaar, W.H., Jonkers, J. (2006). Autotaxin, a secreted lysophospholipase D, is essential for blood vessel formation during development. *Mol Cell Biol*. 26:5015-5022.

26. Mukherjee, P., Hough, G., Chattopadhyay, A., Navab, M., Fogelman, H.R., Meiwether, D., Williams, K., Bensinger, S., Moller, T., Faull, K.F., Lusis, A.J., Iruela-Arispe, M.L., Bostrom, K.I., Tontonoz, P., Reddy, S.T., Fogelman, A.M. (2017) Transgenic tomatoes expressing the 6F peptide and ezetimibe prevent diet-induced increases of IFN-β and cholesterol 25-hydroxylase in jejunum. *J. Lipid Res*. **58**: 1636-1647.

27. Durand, A., Donahue, B., Peignon, G., Letourneur, F., Cagnard, N., Slomianny, C., Perret, C., Shroyer, N.F., and Romagnolo, B. (2012) Functional intestinal stem cells after Paneth cell ablation induced by the loss of transcription factor Math1 (Atoh1). *PNAS* **109**:8965-8970.

28. VanDussen, K.L., Carulli, A.J., Keeley, T.M., Patel, S.R., Puthoff, B.J., Magness, S.T., Tran, I.T., Maillard, I., Siebel, C., Kolterud, A., Grosse, A.S., Gumucio, D.L., Ernst, S.A., Tsai, Y-H., Dempsey, P.J., and Samuelson, L.C. (2012) Notch signaling modulates proliferation and differentiation of intestinal crypt base columnar stem cells. *Development* **139**:488-497.

29. Demitrack, E.S. and Samuelson, L.C. (2016) Notch regulation of gastrointestinal stem cells. *J Phyisol*. **594**:4791-4803.

30. Shroyer, N.F., Wallis, D., Venken, K.J.T., Bellen, H.J. and Zoghbi, H.Y. (2005) *Gfi1* functions downstream of *Math1* to control intestinal secretory cell subtype allocation and differentiation. *Genes & Development* **19**:2412-2417.

31. Ngo, V.L., Abo, H., Maxim, E., Harusato, A., Geem, D., Medina-Contreras, O., Merlin, D., Gewirtz, A.T., Nusrat, A., and Denning, T.L. (2018) A cytokine network involving IL-36γ, IL-23, and IL-22 promotes antimicrobial defense and recovery from intestinal barrier damage. *PNAS* **115**:E5076-E5085.

32. Bohin, N., Keeley, T.M., Carulli, A.J., Walker, E.M., Carlson, E.A., Gao, J., Aifantis, I., Siebel, C.W., Rajala, M.W., Myers, M.G., Jr., Jones, J.C., Brindley, C.D., Dempsey, P.J., and Samuelson, L.C. (2020) Rapid crypt remodeling regenerates the intestinal stem cell niche after Notch inhibition. *Stem Cell Reports* **15**:156-170.

33. Guo, X-K., Ou, J., Liang S., Zhou, X., and Hu, X. (2018) Epithelial Hes1 maintains gut homeostasis by preventing microbial dysbiosis. *Mucosal Immunology*. **11**:716-726.

34. Goldberg, R.F., Austen, W.G., Zhang, X., Munene, G., Mostafa, G., Biswas, S., McCormack, M., Eberlin, K.R., Nguyen, J.T., Tatlidede, H.S., Warren, H.S., Narisawa, S., Millan, J.L., and Hodin, R.A. (2008) Intestinal alkaline phosphatase is a gut mucosal defense factor maintained by enteral nutrition. *PNAS* **105**:3551-3556.

35. Narisawa, S., Huang, L., Iwasaki, A., Hasegawa, H., Alpers, D.H., and Millan, J.L. (2003) Accelerated fat absorption in intestinal alkaline phosphatase knockout mice. *Molecular and Cellular Biology* **23**:7525-7530.

36. Ghosh, S.S., Bie, J., Wang, J. Ghosh S. (2014) Oral supplementation with nonabsorbable antibiotics or curcumin attenuates Western diet-induced atherosclerosis and glucose intolerance in LDLR-/- mice – role of intestinal permeability and macrophage activation. *PLoS One* 9:e108577.

37. Ghosh, S.S., He, H., Wang, J., Korzun, W., Yannie, P.J., Ghosh, S. (2018) Intestine-specific expression of human chimeric intestinal alkaline phosphatase attenuates Western diet-induced barrier dysfunction and glucose intolerance. *Physiol Rep*. 6:e13790.

38. Ghosh, S.S., Wang, J., Yannie, P.J., Ghosh, S. (2020) Intestinal barrier dysfunction, LPS translocation, and disease development. *J Endocr Soc*. 4:1-15.

39. Ghosh, S.S., Wang, J., Yannie, P.J., Cooper, R.C., Sandhu, Y.K., Kakiyama, G., Korzun, W., Ghosh, S. (2021) Over-expression of intestinal alkaline phosphatase attenuates atherosclerosis. *Circ Res*. 128:1646-1659.

40. Ma, J., Liao, X-L., Lou, B., and Wu, M-P. (2004) Role of apolipoprotein A-I in protecting against endotoxin toxicity. *Acta Biochimica et Biophysica Sinica*. **36**:419-424.

41. Beck, W.H.J., Adams, C.P., Biglang-awa, I.M., Patel, A.B., Vincent, H., Haas-Stapleton, E.J. and Weers, P.M.M. (2013) Apolipoprotein A-I binding to anionic vesicles and lipopolysaccharides: role for lysine residues in antimicrobial properties. *Biochimica et Biophysica Acta* **1828**:1503-1510.

42. Salzman, N.H., Underwood, M.A., and Bevins, C.L. (2007) Paneth cells, defensins, and the commensal microbiota: a hypothesis on intimate interplay at the intestinal mucosa. *Semin Immunol*. **19**:70-83.

43. Fahlgren, A., Hammarstrom, S., Danielsson, A., and Hammarstrom, M-L. (2004) β-defensin-3 and-4 in intestinal epithelial cells display increased mRNA expression in ulcerative colitis. *Clin Exp Immunol.* **137**:379-385.

44. Shimizu, H., Okamoto, R., Go, I., Fujii, S., Nakata, T., Suzuki, K., Murano, T., Mizutani, T., Tsuchiya, K., Nakamura, T., Hozumi, K., and Watanabe, M. (2024) Distinct expression patterns of Notch ligands, Dll1 and Dll4, in normal and inflamed mice intestine. *PeerJ*. 2:e370.

45. Mizoguchi, A. (2012) Healing of intestinal inflammation by IL-22. *Inflamm Bowel Dis*. **18**:1777-1784.

46. Shih, V.F-S., Cox, J., Kljavin, N.M., Dengler, H.S., Reichelt, M., Kumar, P., Rangell, L., Kolls, J.K., Diehl, L., Ouyang, W., and Ghilardi, N. (2014) Homeostatic IL-23 receptor signaling limits Th17 response through Il-22-mediated containment of commensal microbiota. *PNAS* **111**:13942-13947.

47. Fatkhullina, A.R., Peshkova, I.O., Dzutsev, A., Aghayev, T., McCulloch, J.A., Thovarai, V., Badger, J.H., Vats, R., Sundd, P., Tang, H-Y., Kossenkov, A.V., Hazen, S.L., Trinchieri, G.,

Grivennikov, S.I., and Koltsova, E.K. (2018) An interleukin-23-interleukin-22 axis regulates intestinal microbial homeostasis to protect from diet-induced atherosclerosis. *Immunity* **49**:943-957.

48. Peeters, T., and Vantrappen, G. (1975) The Paneth cell: A source of intestinal lysozyme. *Gut* 16:553-558.
49. Pelaseyed, T., Bergstrom, J.H., Gustafsson, J.K., Ermund, A., Birchenough, G.M.H., Schutte, A., van der Post, S., Svensson, F., Rodriguez-Pineiro, A.M., Nystrom, E.E.L., Wising, C., Johansson, M.E.V., and Hansson, G.C. (2014) The mucus and mucins of the goblet cells and enterocytes provide the first defense line of the gastrointestinal tract and interact with the immune system. *Immunologic Reviews* **260**:8-20.
50. van Ampting, M.T.J., Loonen, M.P., Schonewille, A.J., Konings, I., Vink, C., Iovanna, J., Chamaillard, M., Dekker, J., van der Meer, R., Wells, J.M., and Bovee-Oudenhoven, I.M. J. (2012) Intestinally secreted C-type lectin Reg3b attenuates salmonellosis but not listeriosis in mice. *Infection and Immunity*. **80**:1115-1120.
51. Vaishnava, S., Yamamoto, M., Severson, K.M., Ruhn, K.A., Yu, X., Koren, O., Ley, R., Wakeland, E.K., and Hooper, L.V. (2011) The antibacterial lectin RegIIIγ promotes the spatial segregation of microbiota and host in the intestine. *Science* **334**: 255-258.
52. Wu, H., Kuzmenko, A., Wan, S., Schaffer, L., Weiss, A., Fisher, J.H., Kim, K.S., and McCormack, F.X. (2003) Surfactant proteins A and D inhibit the growth of gram-negative bacteria by increasing membrane permeability. *J Clin Invest.* **111**:1589-1602.
53. Bals, R., Wang, X., Meegalla, R.L., Wattler, S., Weiner, D.J., Nehls, M.C., and Wilson, J.M. (1999) Mouse β-defensin 3 is an inducible antimicrobial peptide expressed in the epithelia of multiple organs. *Infection and Immunity* **67**:3542-3547.

54. Rahman, A., Fahlgren, A., Sundstedt, C., Hammarstrom, S., Danielsson, A., and Hammarstrom, M.L. (2010) Chronic colitis induces expression of β-defensins in murine intestinal epithelial cells. *Clin Exp Immunol.* **163**:123-130.

55. Hansen, G.H., Rasmussen, K., Niels-Christiansen, L-L., and Danielsen, E.M. (2009) Lipopolysaccharide-binding protein: localization in secretory granules of Paneth cells in mouse small intestine. *Histochem Cell Biol*. **131**:727-732.

56. Vreugdenhil, A.C., Snoek, A.M.P., Greve, J.W.M., and Buurman, W.A. (2000) Lipopolysaccharide-binding protein is vectorially secreted and transported by cultured intestinal epithelial cells and is present in the intestinal mucus of mice. *J Immunol*. **165**:4561-4566.

57. Ito, K., Nakajima, A., Fukushima, Y., Suzuki, K., Sakamoto, K., Hamazaki, Y., Ogasawara, K., Minato, N., and Hattori, M. (2017) The potential role of osteopontin in the maintenance of commensal bacteria homeostasis in the intestine. *PLoS ONE* **12**:e0173629.

58. Nazmi, A., Greer, M.J., Hoek, K.L., Piazuelo, M.B., Weitkamp, J-H., and Olivares-Villagomez, D. (2020) Osteopontin and iCD8α cells promote intestinal intraepithelial lymphocyte homeostasis. *J Immunol.* **204**:1968-1981.

59. Tigyi, G. (2010) Aiming drug discovery at lysophosphatidic acid targets. *British J Pharmacol*. 161:241-270.

60. Su, F., Kozak, K.R., Imaizumi, S., Gao, F., Amneus, M.W., Grijalva, V., Ng, C., Wagner, A., Hough, G., Farias-Eisner, G., Anantharamaiah, G.M., Van Lenten, B.J., Navab, M., Fogelman, A.M., Reddy, S.T., and Farias-Eisner, R. (2010) Apolipoprotein A-I (apoA-I) and apoA-I mimetic peptides inhibit tumor development in a mouse model of ovarian cancer. *PNAS* 107;19997-20002.

61. Dusaulcy, R., Rancoule, C., Gres, S., Wanecq, E., Colom, A., Guigne, C., van Meeteren, L.A., Moolenaar, W.H., Valet, P., and Saulnier-Blache, J.S. (2011) Adipose-specific disruption of

autotaxin enhances nutritional fattening and reduces plasma lysophosphatidic acid. *J Lipid Res*. 52:1247-1255.

62. Brandon, J.A., Kraemer M., Vandra, J., Halder, S., Ubele, M.U., Morris, A.J., and Smyth, S.S. (2019) Adipose-derived autotaxin regulates inflammation and steatosis associated with diet-induced obesity. *PLoS ONE* 14:e0208099.
63. Kraemer, M.P., Mao, G., Hammill, C., Yan, B., Li, Y., Onono, F., Smyth, S.S. and Morris, A.J. (2019) Effects of diet and hyperlipidemia on levels and distribution of circulating lysophosphatidic acid. *J Lipid Res*. 60:1818-1828.
64. Lin, S., Haque, A., Raeman, R., Guo, L., He, P., Denning, T.L, El-Rayes, B., Moolenaar, W.H., and Yun, C.C. (2019) Autotaxin determines colitis severity in mice and is secreted by B cells in the colon. *FASEB J*. 33:3623-3635.
65. Kim, S.J., Howe, C., Mitchell, J., Choo, J., Powers, A., Oikonomopoulos, A., Pothoulakis, C., Hommes, D.W., Im, E., and Rhee, S.H. (2020) Autotaxin loss accelerates intestinal inflammation by suppressing TLR4-mediated immune responses. *EMBO reports* 21:e49332.
66. Karshovska, E., Mohibullah, R., Zhu, M., Zahedi, F., Thomas, D., Magkrioti, C., Geissler, C., Megens, R.T.A., Bianchini M., Nazari-Jahantigh, M., Ferreiros, N., Aidinis, V., Schober, A. (2022) Endothelial ENPP2 (ectonucleotide pyrophosphatase/phosphodiesterase 2) increases atherosclerosis in female and male mice. *Arterioscler Thromb Vasc Biol*. 42:1023-1036.
67. Watson, A.D., Leitinger, N., Navab, M., Faull, K.F., Horkko, S., Witztum, J.L., Palinski, W., Schwenke, D., Salomon, R.G., Sha, W., Subbanagounder, G., Fogelman, A.M., and Berliner, J.A. (1997) Structural identification by mass spectrometry of oxidized phospholipids in minimally oxidized low density lipoprotein that induce monocyte/endothelial interactions and evidence for their presence in vivo. *J. Biol Chem*. 272:13597-13607.
68. Watson, A.D., Subbanagounder, G., Welsbie, D.S., Faull, K.F., Navab, M., Jung, M.E., Fogelman, A.M. and Berliner, J.A. (1999) Structural identification of a novel pro-inflammatory

epoxyisoprostane phospholipid in mildly oxidized low density lipoprotein. *J Biol Chem*. 274:24787-24798.

69. Subbanagounder, G., Leitinger, N., Schwenke, D.C., Wong, J.W., Lee, H., Rizza, C., Watson, A.D., Faull, K.F., Fogelman, A.M. and Berliner, J.A. (2000) Determinants of bioactivity of oxidized phospholipids. Specific oxidized fatty acyl groups at the sn-2 position. *Arterioscler Thromb Vasc Biol.* 20:2248-2254.
70. Navab, M., Berliner, J.A., Subbanagounder, G., Hama, S., Lusis, A.J., Castellani, L.W., Reddy, S., Shih, D., Shi, W., Watson, A.D., Van Lenten, B. J., Vora, D., Fogelman, A.M. (2001) HDL and the inflammatory response induced by LDL-derived oxidized phospholipids. *Arterioscler Thromb Vasc Biol.* 21:481-488.
71. Smyth, S.S., Mueller, P., Yang, F., Brandon, J.A., Morris A.J. (2014) Arguing the case for the autotaxin-lysophosphatidic acid-lipid phosphate phosphatase-3-signaling nexus in the development and complications of atherosclerosis. *Arterioscler Thromb Vasc Biol*. 34:479-486.

FIGURE LEGENDS

Figure 1. *Enpp2* gene expression and autotaxin protein levels in jejunum. **A.** *Enpp2* gene expression after feeding a chow diet (Chow) or Western diet (WD) for two weeks. Female *Enpp2$^{fl/fl}$/Ldlr$^{-/-}$* (Cont.) mice 3.1 ± 0.4 months of age (n = 5 mice per group) and female *Enpp2$^{fl/fl}$/Ldlr$^{-/-}$/VilCre* (iKO) mice 3.9 ± 0.4 months of age (n = 5 mice per group) were fed either Chow or WD. After two weeks, enterocytes were isolated from the jejunum, and *Enpp2* gene expression was determined by RT-qPCR as described in Methods. **B.** *Enpp2* gene expression after feeding Chow or WD for five months. Female Cont. mice, 2.6 ± 0.1 months of age (n = 5 mice per group), and female iKO mice 2.8 ± 0.1 months of age (n = 5 mice per group) were fed either Chow or WD. After five months, enterocytes were isolated from the jejunum, and *Enpp2* gene expression was determined by RT-qPCR as described in Methods. **C.** Enterocyte autotaxin protein increased on WD in Cont. mice but not in iKO mice. Female Cont. mice or female iKO mice 4 to 5 months of age (n = 8 per group) were fed Chow or WD. After two weeks, enterocytes were prepared

and highly purified by flow cytometry, the levels of autotaxin protein in the enterocytes were determined by Western blot analysis and normalized to vinculin as described in Methods. * $P < 0.05$; ** $P < 0.01$; *** $P < 0.001$; **** $P < 0.0001$.

Figure 2. Lysophosphatidic acid levels in enterocytes. Male *Enpp2*$^{fl/fl}$*/Ldlr*$^{-/-}$ (Cont.) mice 6.1 ± 0.2 months of age (n = 18 mice per group) and male *Enpp2*$^{fl/fl}$*/Ldlr*$^{-/-}$*/VilCre* (iKO) mice 6.2 ± 0.1 months of age (n = 18 mice per group) were fed either the chow diet (Chow) or the Western diet (WD). After two weeks, enterocytes were isolated from the jejunum, and LPA levels were determined as described in Methods. **A.** LPA 16:0. **B.** LPA 18:0. **C.** LPA 18:1. **D**. LPA 18:2. * $P < 0.05$; *** $P < 0.001$; **** $P < 0.0001$.

Figure 3. Oxidized phospholipids in jejunum mucus. Female *Enpp2*$^{fl/fl}$*/Ldlr*$^{-/-}$ (Cont.) mice 3.5 ± 0.3 months of age (n = 10 mice per group) and female *Enpp2*$^{fl/fl}$*/Ldlr*$^{-/-}$*/VilCre* (iKO) mice 3.5 ± 0.3 months of age (n = 10 mice per group) were fed either the chow diet (Chow) or the Western diet (WD). After two weeks, jejunum mucus was collected and the levels of oxidized phospholipids were determined by E06 ELISA as described in Methods. * $P < 0.05$; *** $P < 0.001$.

Figure 4. Nineteen genes that directly or indirectly regulate the levels of intestinal antimicrobial peptides and proteins were selected for study. Female *Enpp2*$^{fl/fl}$*/Ldlr*$^{-/-}$ (Cont.) mice 3.3 ± 0.3 months of age (n = 10 mice per group) and female *Enpp2*$^{fl/fl}$*/Ldlr*$^{-/-}$*/VilCre* (iKO) mice 3.4 ± 0.3 months of age (n = 10 mice per group) were fed either the chow diet (Chow) or the Western diet (WD). After two weeks, enterocytes were isolated from the jejunum of the mice and gene expression for these 19 genes was determined by RT-qPCR as described in Methods. The data are presented as a heat map, which compares the expression of each gene to that in Cont. mice on a chow diet. **A.** the results are shown for 17 genes whose expression was previously reported to have decreased in the jejunum of *Ldlr*$^{-/-}$ mice fed a WD (22): intestinal alkaline phosphatase (*Alp1*) (34-39); apolipoprotein A-I (*ApoA*-I) (40,41); atonal homolog 1 (*Atoh1*) (27-29); Defensin 4 (*Defb4*) (42,43); delta like canonical notch ligand 4 (*Dll4*) (44); growth factor independent protein 1 (*Gfi1*) (30); interleukin 22 (*Il22*) (31,45); interleukin 23 (*Il23*) (31,46,47); interleukin 36γ

(*Il36γ*) (31); lysozyme (*Lyz*) (48); mucin 2 (*Muc2*) (49); notch receptor 1 (*Notch1*) (33); notch receptor 2 (*Notch2*) (31); regenerating islet-derived 3b (*Reg3b*) (50); regenerating islet-derived 3g (*Reg3g*) (51); surfactant A (*Sftpa1*) (52); defensin 3 (*Defb3*) (53,54). **B.** the results are shown for two genes whose expression was previously reported to have increased in the jejunum of *Ldlr*$^{-/-}$ mice fed a WD (22): lipopolysaccharide-binding protein (*Lbp*) (55,56); secreted phosphoprotein 1 (*Spp1*) (57,58). Statistical analysis of the data in Figure 4 is shown in Supplemental Table S3.

Figure 5. Quantification of atonal homolog 1 (ATOH1) and growth factor independent protein 1 (GFI1) by ELISA and quantification of goblet and Paneth cells in jejunum by immunohistochemistry. **A.** Female *Enpp2*$^{fl/fl}$*/Ldlr*$^{-/-}$ (Cont.) mice 3.3 ± 0.2 months of age (n = 12 mice per group) and female *Enpp2*$^{fl/fl}$*/Ldlr*$^{-/-}$*/VilCre* (iKO) mice 3.5 ± 0.2 months of age (n = 12 mice per group) were fed either the chow diet (Chow) or the Western diet (WD). After two weeks, the levels of ATOH1 in jejunum was determined by ELISA as described in Methods. **B.** Male Cont. mice 6.9 ± 0.5 months of age (n = 12 mice per group) and male iKO mice 7.0 ± 0.5 months of age (n = 12 mice per group) were fed either Chow or WD. After two weeks, the levels of GFI1 in jejunum was determined by ELISA as described in Methods. **C**. Male Cont. mice 6 weeks of age (n = 3 mice per group) and male iKO mice 6 weeks of age (n = 3 mice per group) were fed either Chow or WD. After two weeks, the number of goblet cells/villus was determined as described in Methods. **D**. The number of goblet cells/crypt was determined in the mice in C as described in Methods. **E.** The number of Paneth cells/crypt was determined in the mice in C as described in Methods. * $P < 0.05$; ** $P < 0.01$; *** $P < 0.001$; **** $P < 0.0001$.

Figure 6. Quantification of Interleukin 36γ (IL-36 γ), Interleukin 23 (IL-23), Interleukin 22 (IL-22), Lysozyme and Mucin2 (MUC2) by ELISA. **A.** IL-36 γ and **B.** IL-23 levels in the jejunums of the mice described in Figure 5B [Male *Enpp2*$^{fl/fl}$*/Ldlr*$^{-/-}$ (Cont.) mice 6.9 ± 0.5 months of age (n = 12 mice per group) and male *Enpp2*$^{fl/fl}$*/Ldlr*$^{-/-}$*/VilCre* (iKO) mice 7.0 ± 0.5 months of age (n = 12 mice per group)] were fed either the chow diet (Chow) or the Western diet (WD). After two weeks, the levels of IL-36 γ and IL-23 were determined by ELISA as described in Methods. **C.** Male Cont. mice 6.5 ± 0.4 months

of age (n = 16 mice per group) and male iKO mice 6.9 ± 0.5 months of age (n = 16 mice per group) were fed either Chow or WD. After two weeks, the levels of IL-22 in jejunum was determined by ELISA as described in Methods. **D.** Lysozyme and **E.** MUC2 levels in jejunum mucus from the mice in panels A and B were determined by ELISA as described in Methods. * $P < 0.05$; *** $P < 0.001$; **** $P < 0.0001$.

Figure 7. Quantification of NOTCH2, DLL4, APOA-I and LBP by ELISA. Male *Enpp2$^{fl/fl}$/Ldlr$^{-/-}$* (Cont.) mice 6.5 ± 0.4 months of age (n = 16 mice per group) and male *Enpp2$^{fl/fl}$/Ldlr$^{-/-}$/VilCre* (iKO) mice 6.9 ± 0.5 months of age (n = 16 mice per group) were fed either the chow diet (Chow) or the Western diet (WD). After two weeks, jejunum levels of NOTCH2 (**A**) or DLL4 (**B**) were determined by ELISA as described in Methods. **C.** Male Cont. mice 7.4 ± 0.3 months of age (n = 8 mice per group) and male iKO mice 7.4 ± 0.3 months of age (n = 8 mice per group) were fed either Chow or WD. After two weeks, the levels of APOA-I in jejunum mucus was determined by ELISA as described in Methods. **D.** Female Cont. mice 3.4 ± 0.3 months of age (n = 12 mice per group) and female iKO mice 3.3 ± 0.3 months of age (n = 12 mice per group) were fed either Chow or WD. After two weeks, the levels of LBP in jejunum mucus were determined by ELISA as described in Methods. * $P < 0.05$; ** $P < 0.01$; *** $P < 0.001$; **** $P < 0.0001$.

Figure 8. LPS levels increased in jejunum mucus on the Western diet (WD), but increased much less in the *Enpp2$^{fl/fl}$/Ldlr$^{-/-}$/VilCre* (iKO) mice. Female *Enpp2$^{fl/fl}$/Ldlr$^{-/-}$* (Cont.) mice 3.3 ± 0.3 months of age (n = 12 mice per group) and female iKO mice 3.4 ± 0.3 months of age (n = 12 mice per group) were fed either the chow diet (Chow) or WD. After two weeks, LPS levels were determined in jejunum mucus as described in Methods. * $P < 0.05$; ** $P < 0.01$; **** $P < 0.0001$.

Figure 9. Plasma total cholesterol, triglycerides and apoA-I after two weeks on the chow diet (Chow) or the Western diet (WD). The mice described in Figure 5A [Female *Enpp2$^{fl/fl}$/Ldlr$^{-/-}$* (Cont.) mice 3.3 ± 0.2 months of age (n = 12 mice per group) and female *Enpp2$^{fl/fl}$/Ldlr$^{-/-}$/VilCre* (iKO) mice 3.5 ± 0.2 months of age (n = 12 mice per group)] were fed either Chow or WD. After two weeks, plasma levels of total

cholesterol (**A**), triglycerides (**B**) and apoA-I (**C**) were determined as described in Methods. ** $P < 0.01$; *** $P < 0.001$; **** $P < 0.0001$

Figure 10. Plasma LPA levels after two weeks on the chow diet (Chow) or the Western diet (WD). The mice described in Figure 5A [Female *Enpp2*$^{fl/fl}$*/Ldlr*$^{-/-}$ (Cont.) mice 3.3 ± 0.2 months of age (n = 12 mice per group) and female *Enpp2*$^{fl/fl}$*/Ldlr*$^{-/-}$*/VilCre* (iKO) mice 3.5 ± 0.2 months of age (n = 12 mice per group])] were fed either Chow or WD. After two weeks, plasma levels of LPA 16:0 (**A**), LPA 18:0 (**B**), LPA 18:1(**C**) and LPA 18:2 (**D**) were determined as described in Methods. * $P < 0.05$; ** $P < 0.01$.

Figure 11. Plasma levels of LBP, LPS, IL-6 and SAA after two weeks on the chow diet (Chow) or the Western diet (WD). The mice described in Figure 5A [Female *Enpp2*$^{fl/fl}$*/Ldlr*$^{-/-}$ (Cont.) mice 3.3 ± 0.2 months of age (n = 12 mice per group) and female *Enpp2*$^{fl/fl}$*/Ldlr*$^{-/-}$*/VilCre* (iKO) mice 3.5 ± 0.2 months of age (n = 12 mice per group)] were fed either Chow or WD. After two weeks, plasma levels of LBP (**A**), LPS (**B**), IL-6 (**C**) and SAA (**D**) were determined as described in Methods. * $P < 0.05$; *** $P < 0.001$; **** $P < 0.0001$.

Figure 12. Plasma LBP, LPS and SAA after five months on the chow diet (Chow) or the Western diet (WD). The mice described in Supplemental Figure S7 [Female *Enpp2*$^{fl/fl}$*/Ldlr*$^{-/-}$ (Cont.) mice 2.6 ± 0.1 months of age (n = 19 to 20 mice per group) and female *Enpp2*$^{fl/fl}$*/Ldlr*$^{-/-}$*/VilCre* (iKO) mice 2.8 ± 0.1 months of age (n = 18 to 20 mice per group)] were fed either Chow or WD. After five months, plasma levels of LBP (**A**), LPS (**B**), and SAA (**C**) were determined as described in Methods. * $P < 0.05$; ** $P < 0.01$; *** $P < 0.001$; **** $P < 0.0001$.

Figure 13. Aortic lesions after five months on the chow diet (Chow) or the Western diet (WD). The mice described in Supplemental Figure S7 [Female *Enpp2*$^{fl/fl}$*/Ldlr*$^{-/-}$ (Cont.) mice 2.6 ± 0.1 months of age (n = 19 to 20 mice per group) and female *Enpp2*$^{fl/fl}$*/Ldlr*$^{-/-}$*/VilCre* (iKO) mice 2.8 ± 0.1 months of age (n = 18 to 20 mice per group)] were fed either Chow or WD. After five months the extent of aortic atherosclerosis was determined as the percent of aorta with lesions (**A**), or the lesion area in the aortic root was

determined by Oil Red O staining (**B**), or the area staining for CD68 was determined (**C**) as described in Methods. ** $P < 0.01$; **** $P < 0.0001$.

Figure 14. A schematic diagram showing that i) feeding a Western diet to *Ldlr*$^{-/-}$ mice increases reactive oxygen species (ROS) in intestine that ii) promote the formation of oxidized phospholipids in intestine, which iii) induce *Enpp2* and raise autotaxin levels in enterocytes, that iv) increases enterocyte lysophosphatidic acid (LPA) levels, that v) feedback to promote intestinal formation of ROS that maintain the high levels of intestinal oxidized phospholipids, that vi) decrease the levels of antimicrobial peptides and proteins in the intestine, that vii) lead to elevated levels of gut-derived lipopolysaccharide (LPS) in plasma, that viii) enhance dyslipidemia, systemic inflammation, and atherosclerosis.

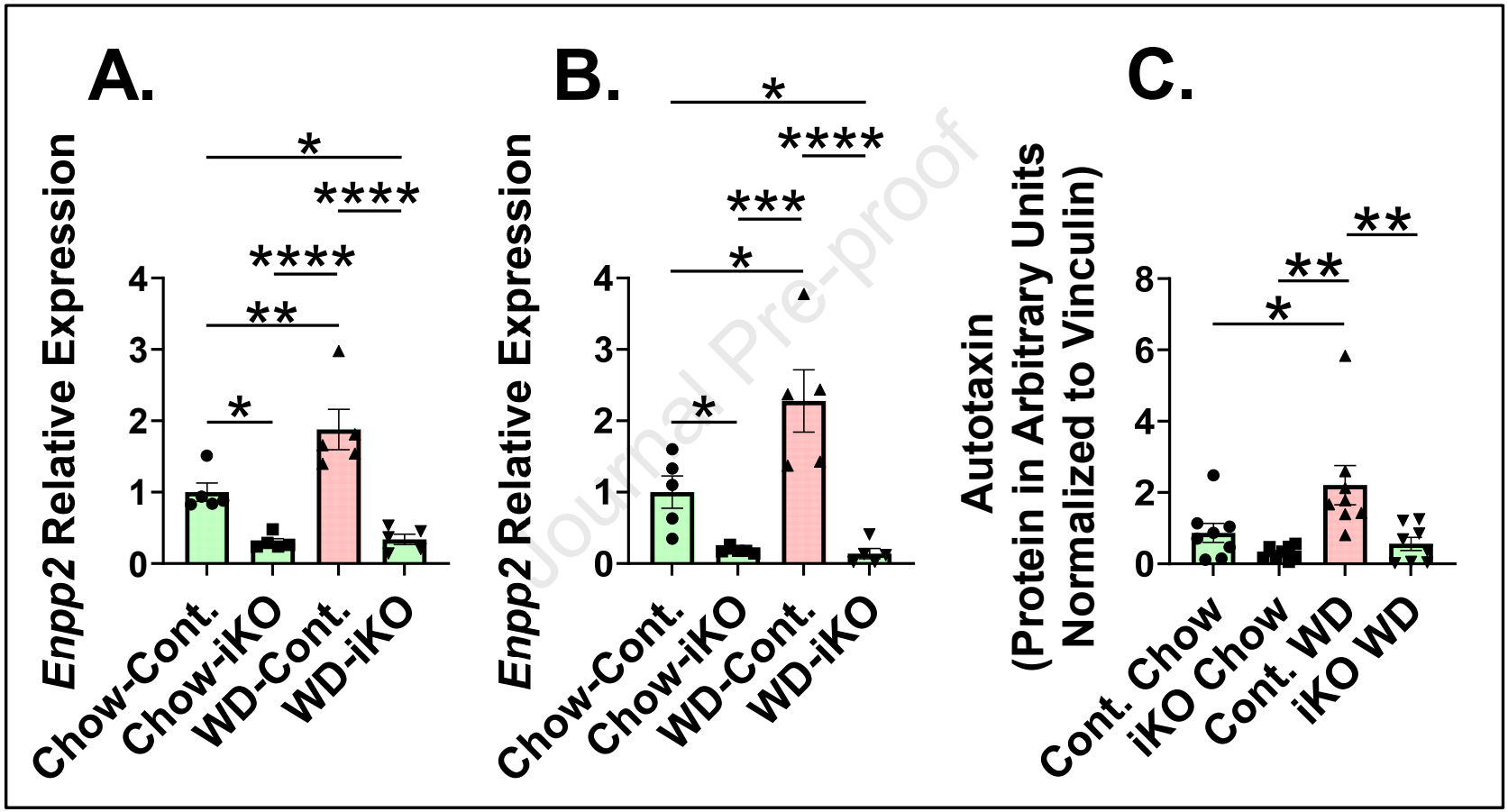

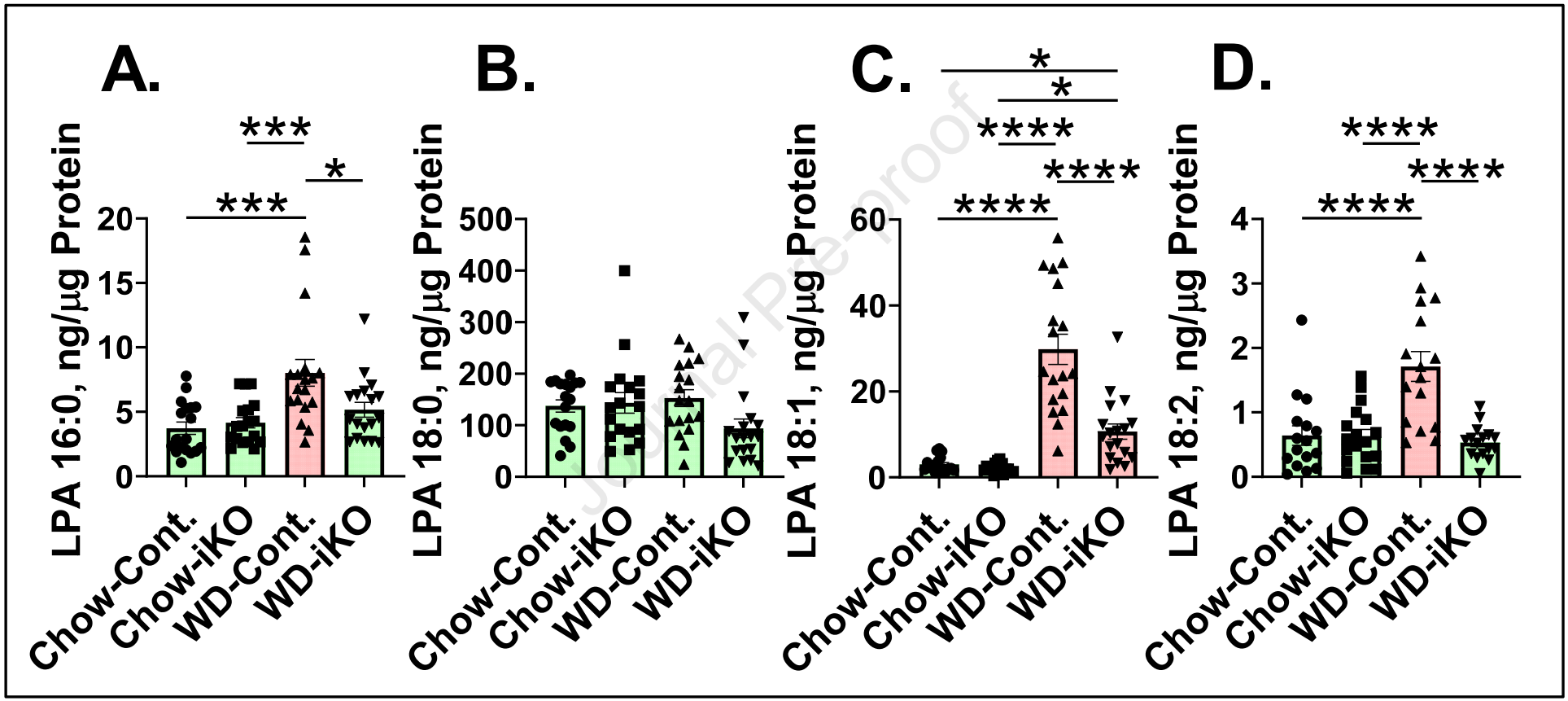

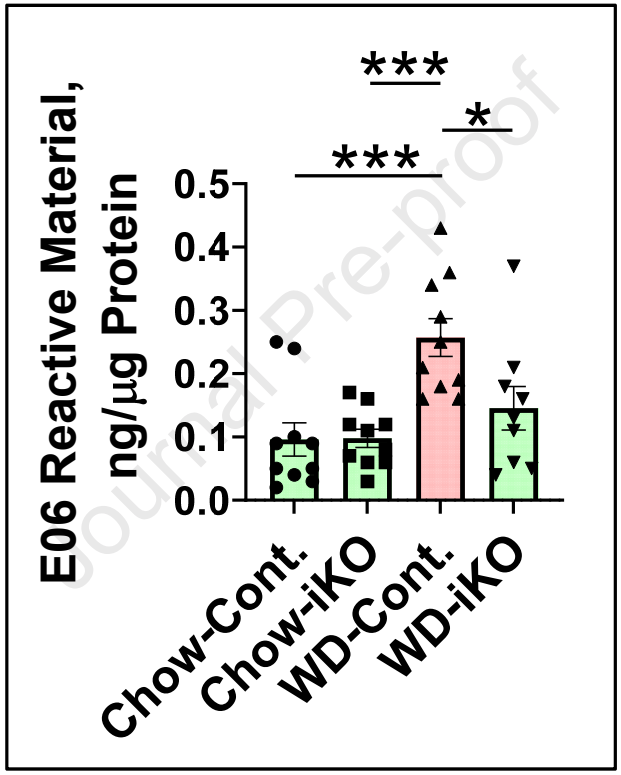

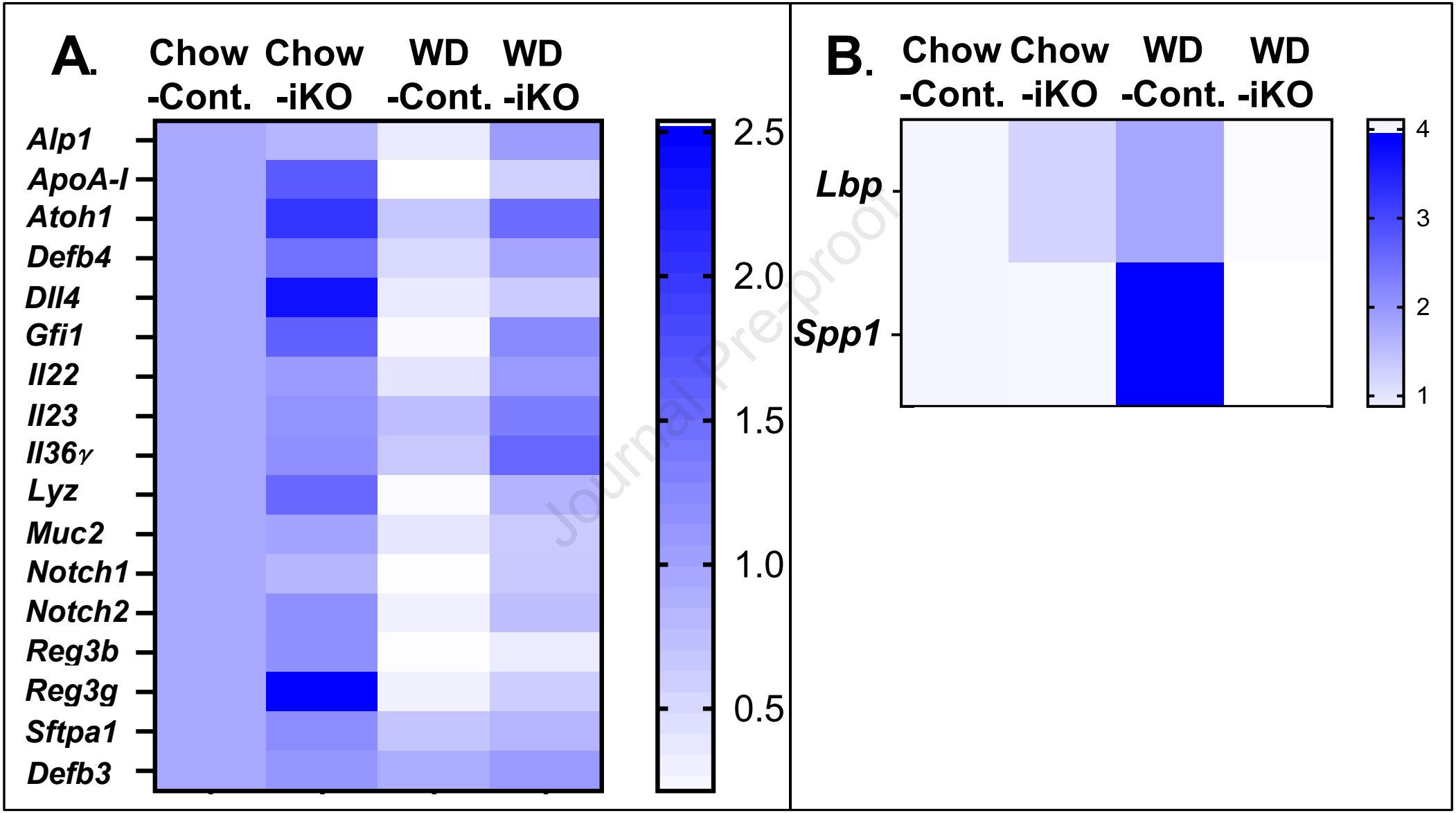

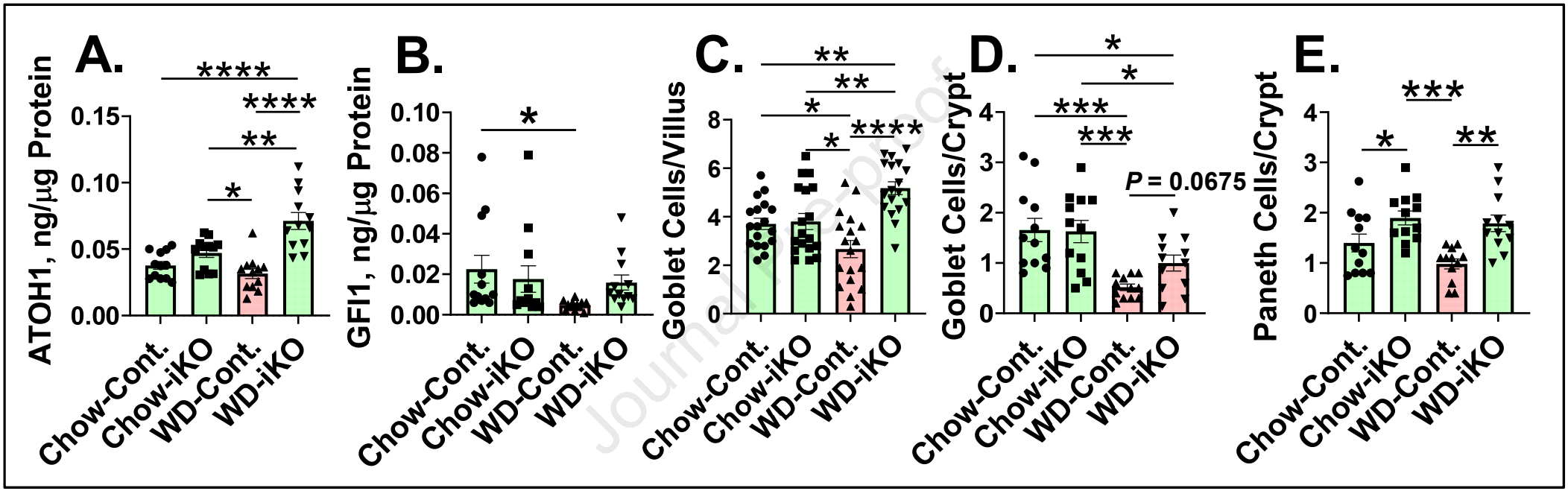

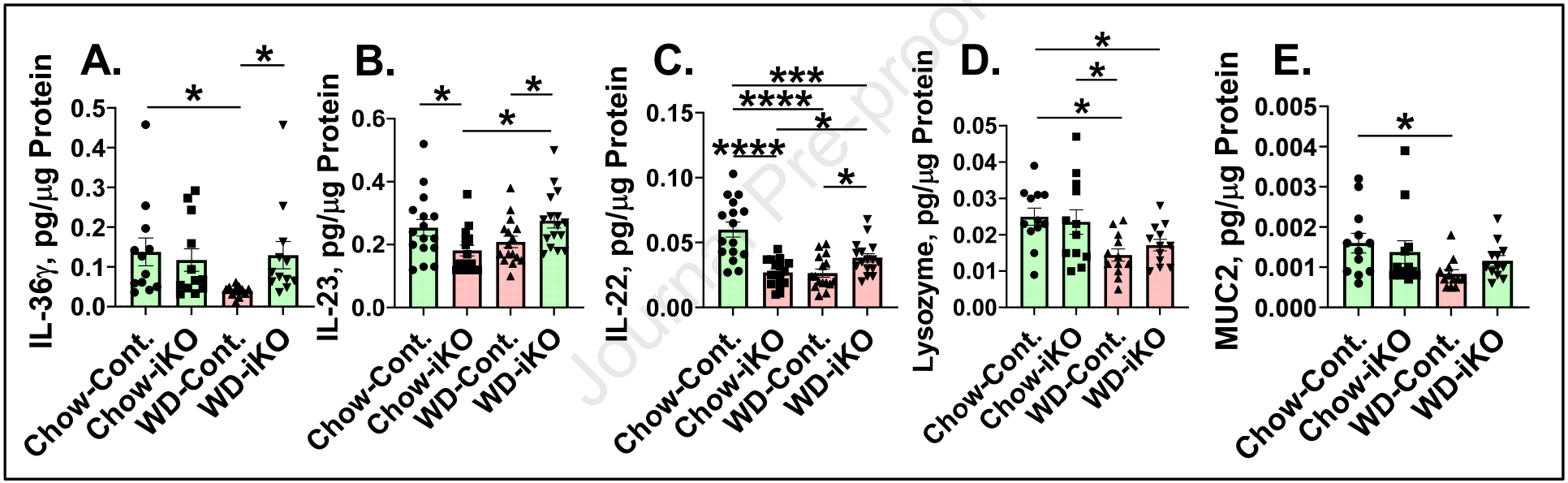

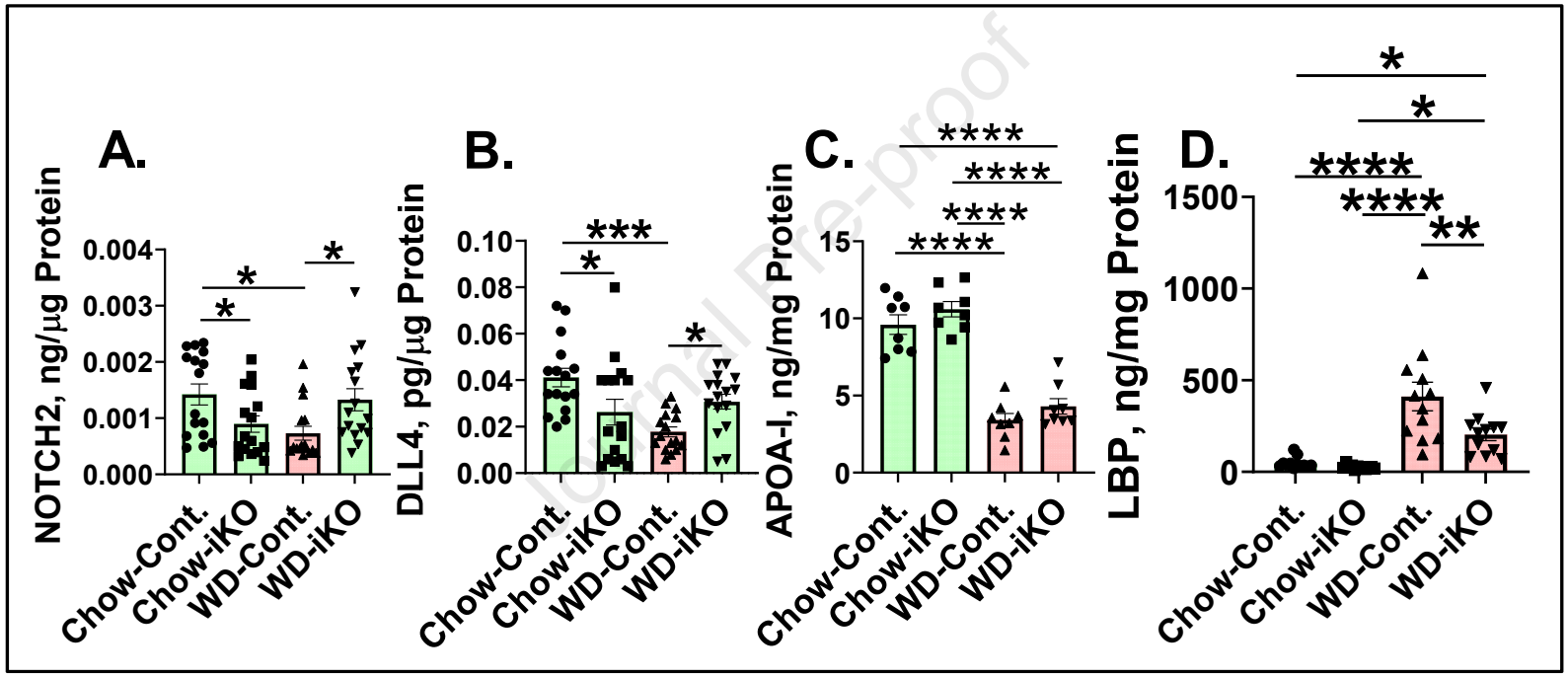

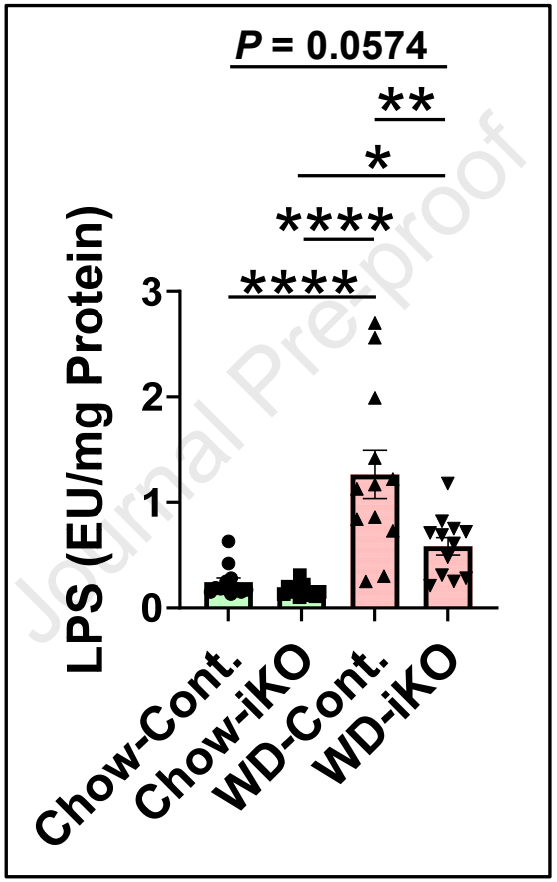

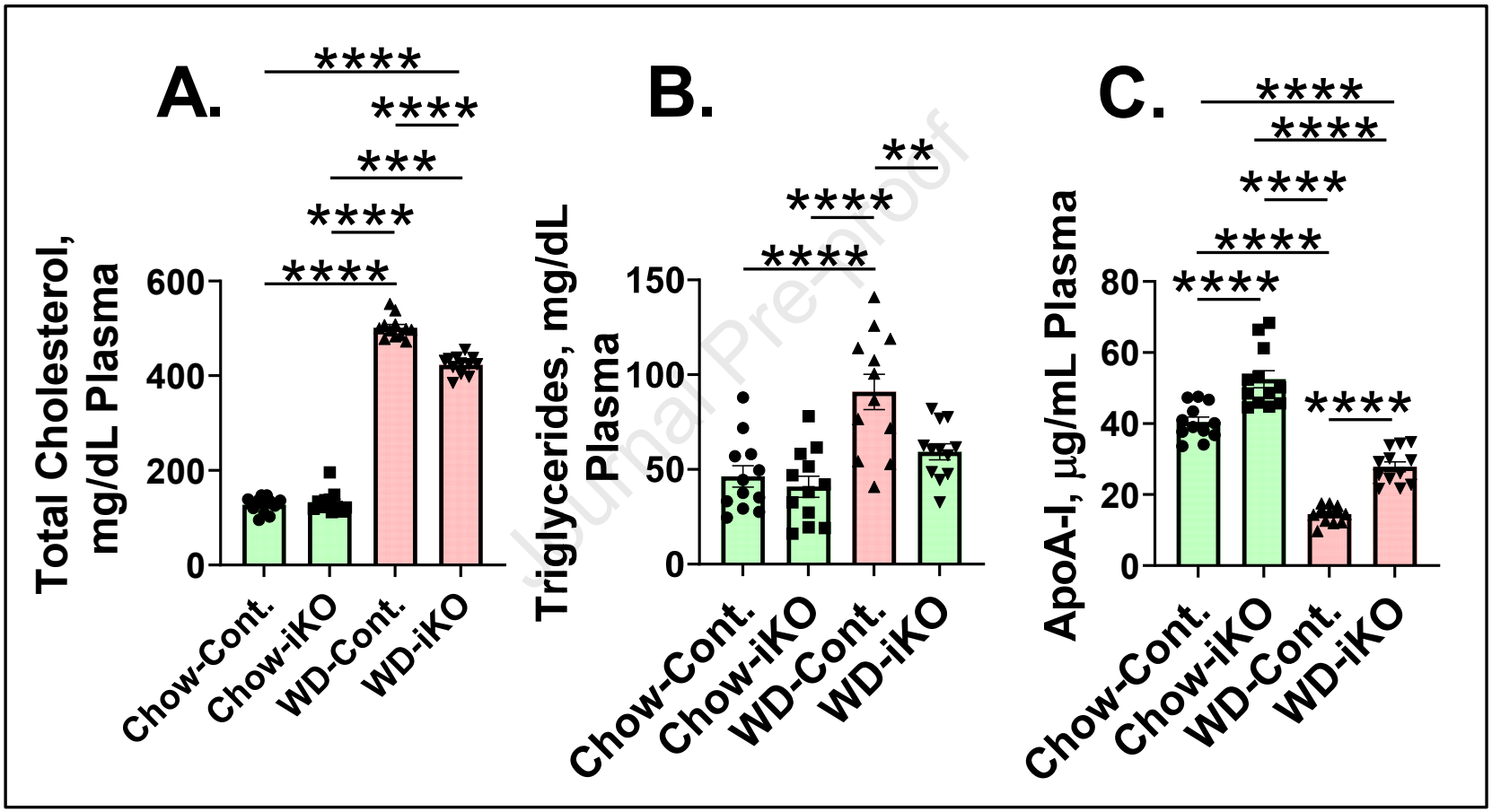

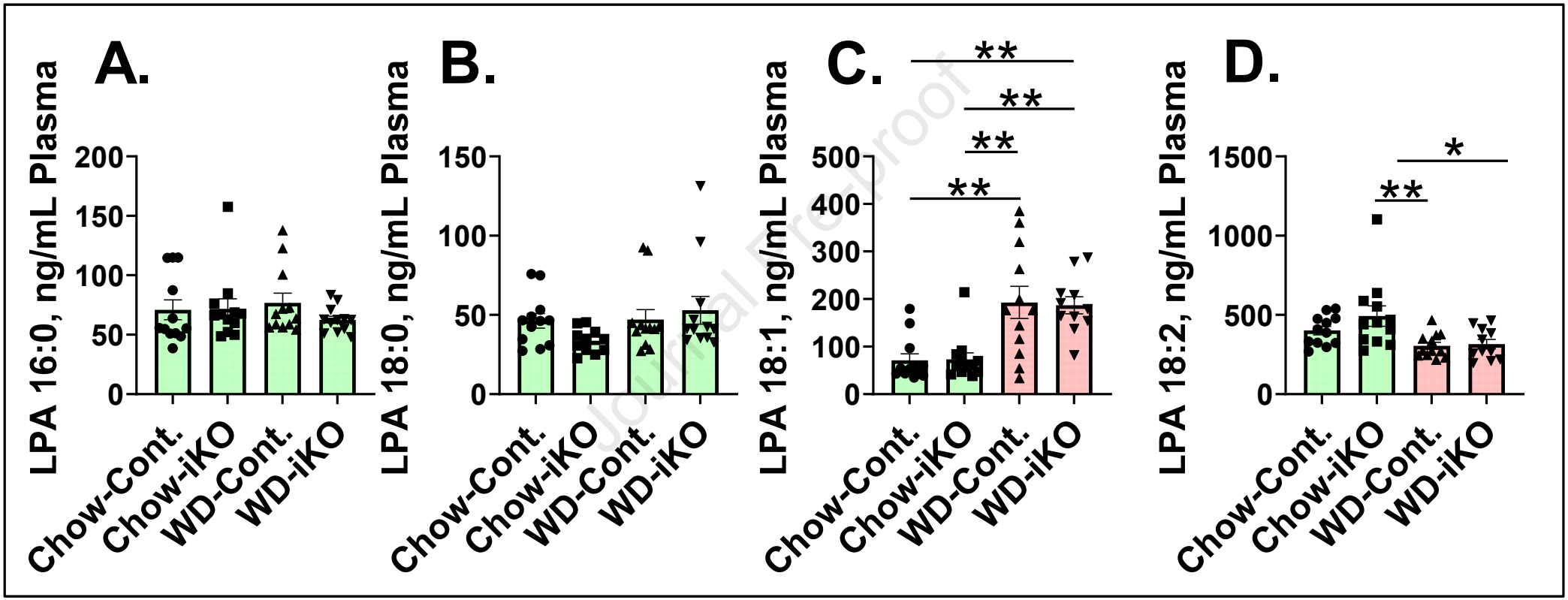

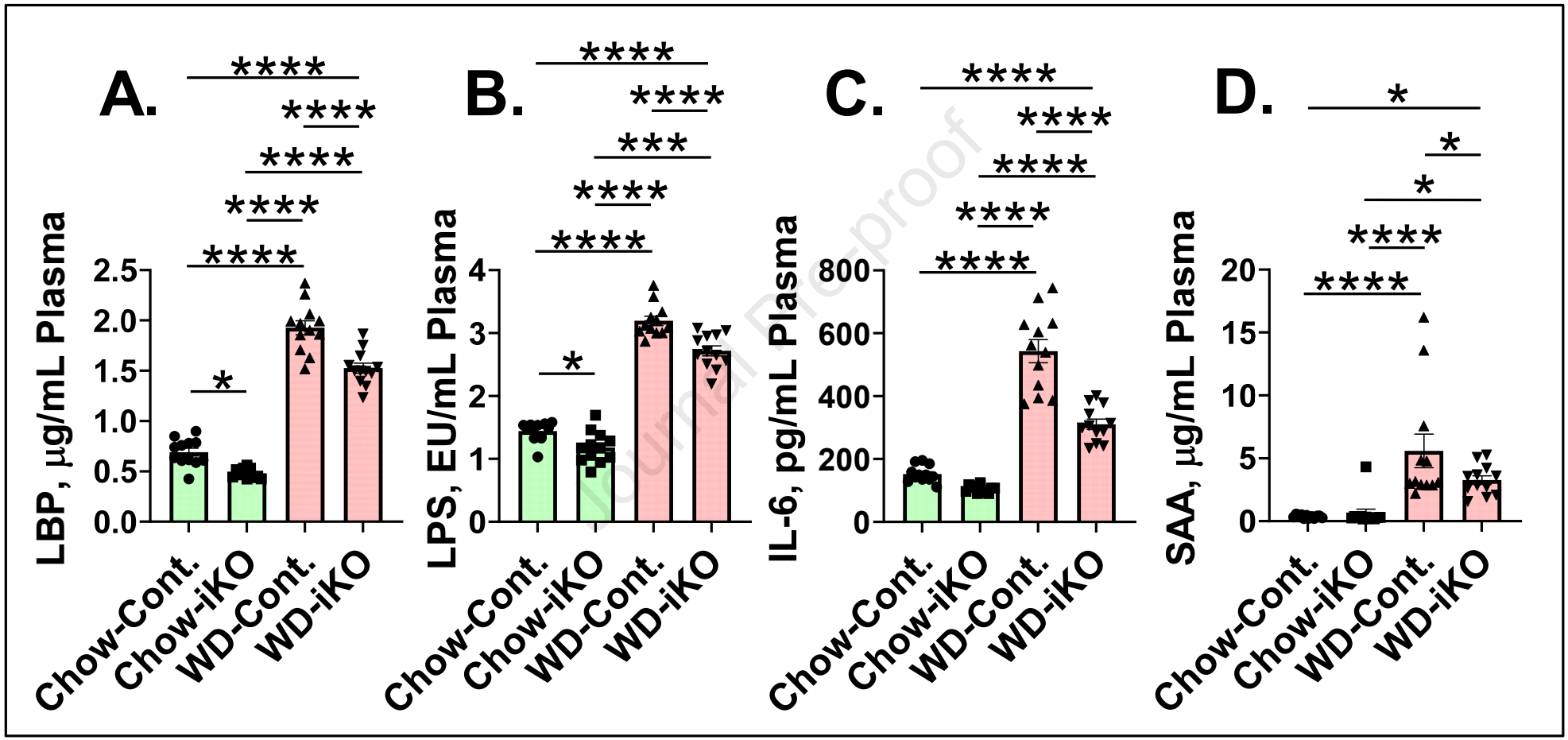

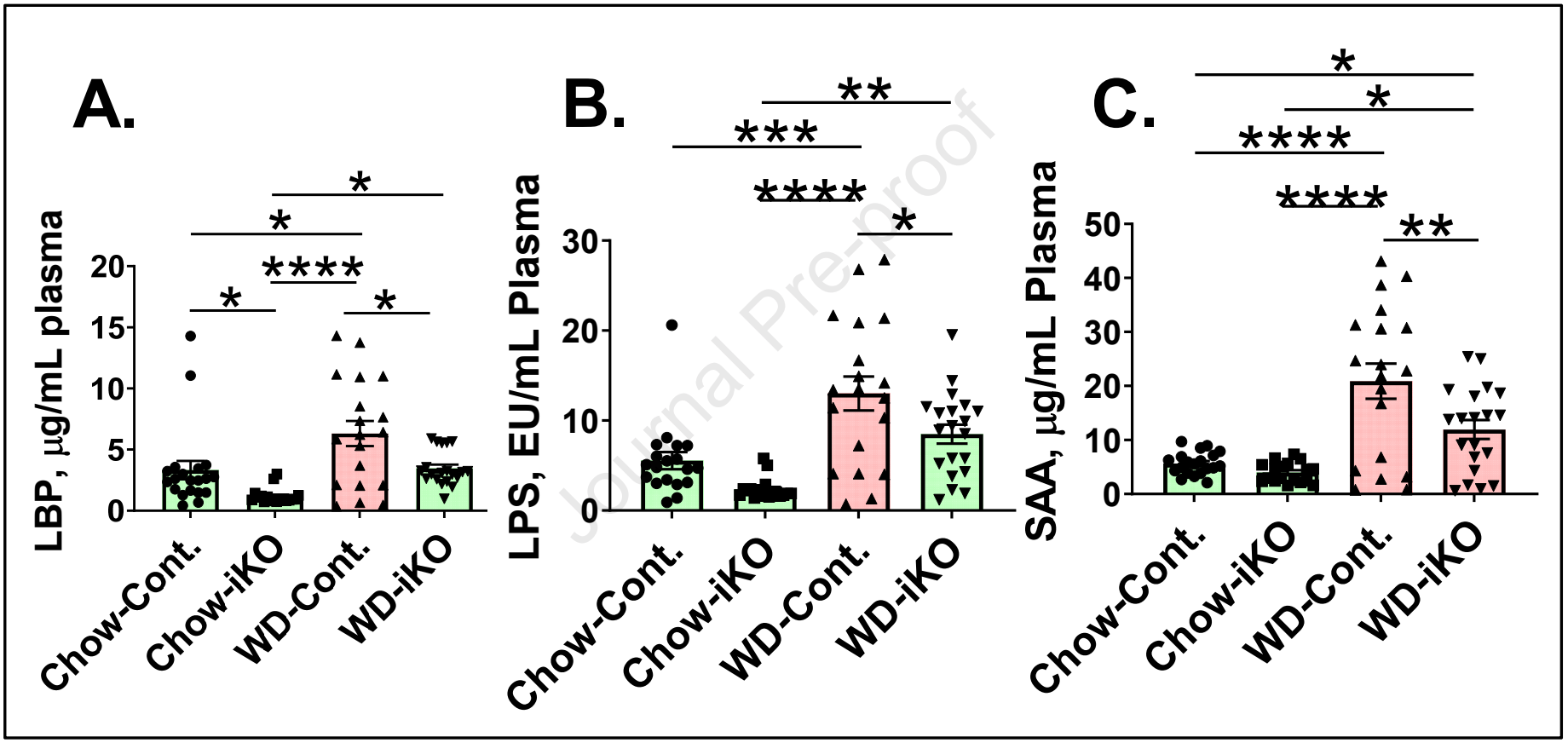

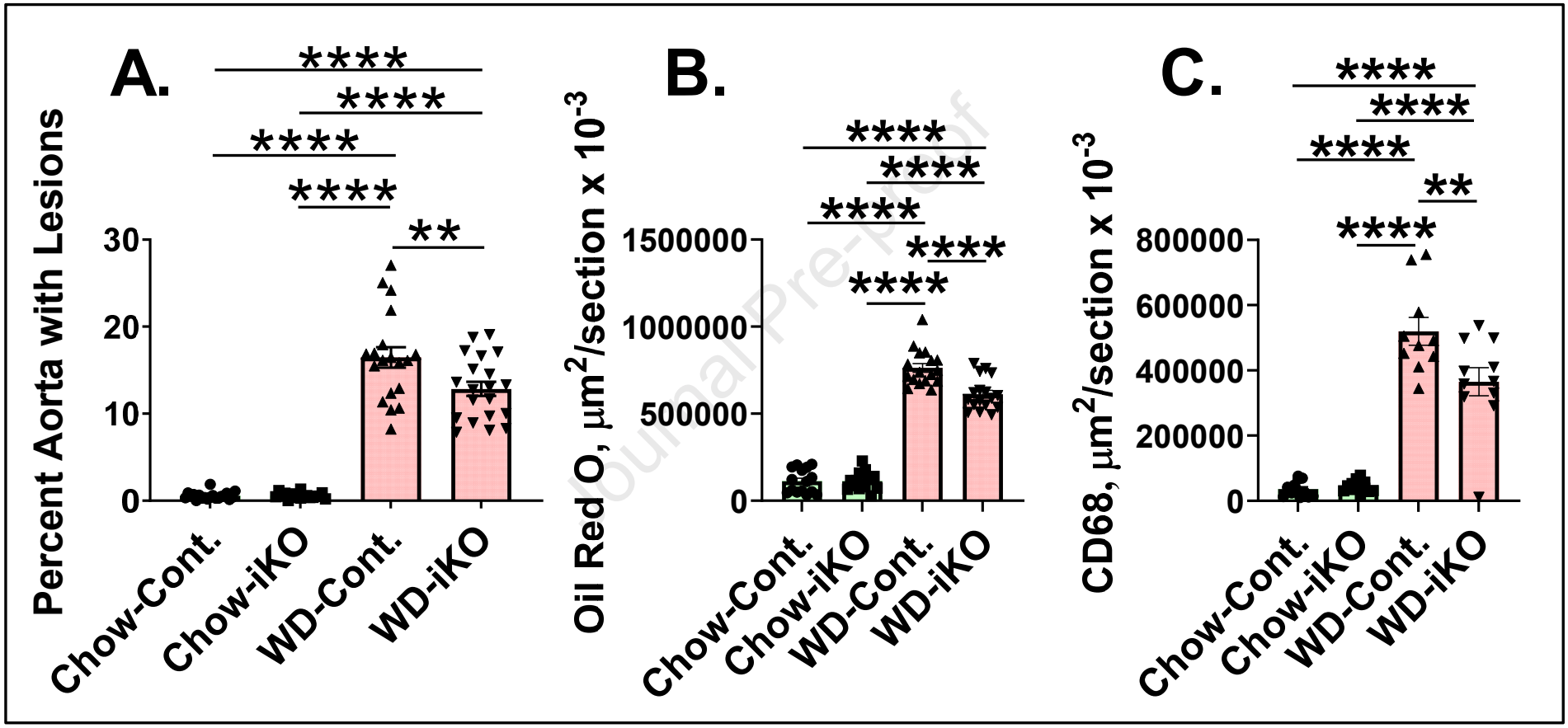

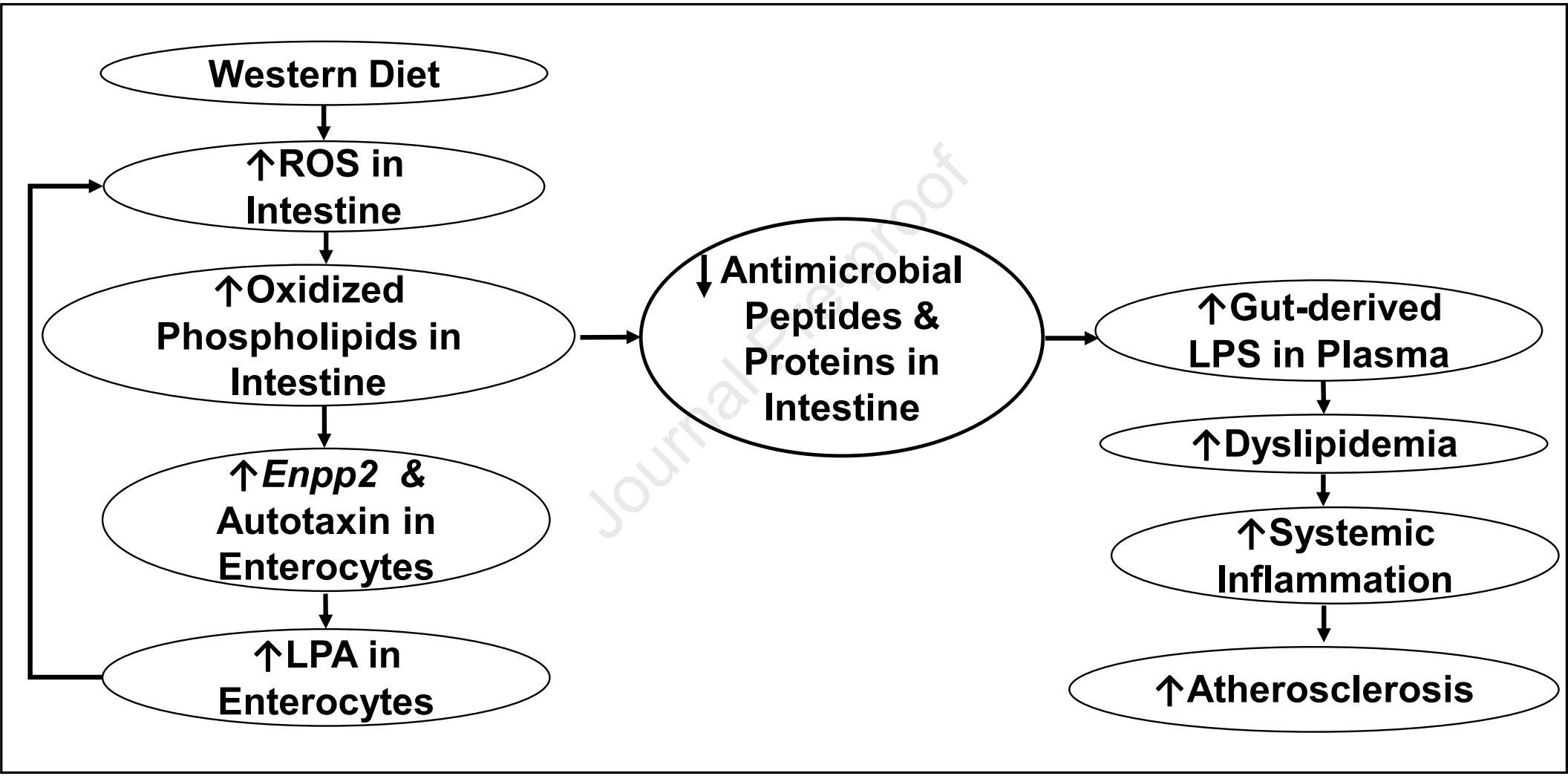

Investigation, Formal Analysis, Data Curation, Writing **Arnab Chattopadhyay**

Investigation, Conceptualization **Pallavi Mukherjee**

Investigation **Dawoud Sulaiman**

Investigation **Huan Wang**

Investigation Victor Girjalva

Formal Analysis **Nasrin Dorreh**

Resources **Jonathan P. Jacobs**

Formal Analysis **Samuel Delk**

Methodology **Wouter H. Moolenaar**

Review **Mohamad Navab**

Conceptualization, Project Administration, Supervision, Writing, Visualization **Srinivasa T. Reddy**

Conceptualization, Formal Analysis, Funding Acquisition, Project Administration, Writing, Visualization **Alan M. Fogelman**